





Article

Multi-Objective Energy Management and Charging Strategy for Electric Bus Fleets in Cities Using Various ECO Strategies

Mohammed Mahedi Hasan ^{1,2,*} , Nikos Avramis ³, Mikaela Ranta ⁴, Andoni Saez-de-Ibarra ⁵ ,
Mohamed El Baghdadi ^{1,2}  and Omar Hegazy ^{1,2} 

¹ ETEC Department & MOBI Research Group, Vrije Universiteit Brussel, 1050 Brussels, Belgium; mohamed.el.baghdadi@vub.be (M.E.B.); Omar.Hegazy@vub.be (O.H.)

² Flanders Make, 3001 Heverlee, Belgium

³ TNO Automotive, Automotive Campus 30, 5708 JZ Helmond, The Netherlands; nikos.avramis@tno.nl

⁴ VTT Technical Research Center, Vuorimiehentie 3, P.O. Box 1000, 02044 Espoo, Finland; mikaela.ranta@vtt.fi

⁵ Ikerlan Technology Research Centre, Basque Research and Technology Alliance (BRTA), 20500 Gipuzkoa, Spain; asaezdeibarra@ikerlan.es

* Correspondence: Mohammed.Mahedi.Hasan@vub.be; Tel.: +32-466-303-546

Abstract: The paper presents use case simulations of fleets of electric buses in two cities in Europe, one with a warm Mediterranean climate and the other with a Northern European (cool temperate) climate, to compare the different climatic effects of the thermal management strategy and charging management strategy. Two bus routes are selected in each city, and the effects of their speed, elevation, and passenger profiles on the energy and thermal management strategy of vehicles are evaluated. A multi-objective optimization technique, the improved Simple Optimization technique, and a “brute-force” Monte Carlo technique were employed to determine the optimal number of chargers and charging power to minimize the total cost of operation of the fleet and the impact on the grid, while ensuring that all the buses in the fleet are able to realize their trips throughout the day and keeping the battery SoC within the constraints designated by the manufacturer. A mix of four different types of buses with different battery capacities and electric motor specifications constitute the bus fleet, and the effects that they have on charging priority are evaluated. Finally, different energy management strategies, including economy (ECO) features, such as ECO-comfort, ECO-driving, and ECO-charging, and their effects on the overall optimization are investigated. The single bus results indicate that 12 m buses have a significant battery capacity, allowing for multiple trips within their designated routes, while 18 m buses only have the battery capacity to allow for one or two trips. The fleet results for Barcelona city indicate an energy requirement of 4.42 GWh per year for a fleet of 36 buses, while for Gothenburg, the energy requirement is 5 GWh per year for a fleet of 20 buses. The higher energy requirement in Gothenburg can be attributed to the higher average velocities of the bus routes in Gothenburg, compared to those of the bus routes in Barcelona city. However, applying ECO-features can reduce the energy consumption by 15% in Barcelona city and by 40% in Gothenburg. The significant reduction in Gothenburg is due to the more effective application of the ECO-driving and ECO-charging strategies. The application of ECO-charging also reduces the average grid load by more than 10%, while shifting the charging towards non-peak hours. Finally, the optimization process results in a reduction of the total fleet energy consumption of up to 30% in Barcelona city, while in Gothenburg, the total cost of ownership of the fleet is reduced by 9%.

Keywords: simulation framework; ECO-charging; ECO-driving; ECO-comfort; TMS; EMS; CMS; E-bus fleet; total cost of ownership; iSOPT; Monte Carlo



Citation: Hasan, M.M.; Avramis, N.; Ranta, M.; Saez-de-Ibarra, A.; El Baghdadi, M.; Hegazy, O.

Multi-Objective Energy Management and Charging Strategy for Electric Bus Fleets in Cities Using Various ECO Strategies. *Sustainability* **2021**, *13*, 7865. <https://doi.org/10.3390/su13147865>

Academic Editor: Mouloud Denai

Received: 4 June 2021

Accepted: 7 July 2021

Published: 14 July 2021

Publisher's Note: MDPI stays neutral with regard to jurisdictional claims in published maps and institutional affiliations.



Copyright: © 2021 by the authors. Licensee MDPI, Basel, Switzerland. This article is an open access article distributed under the terms and conditions of the Creative Commons Attribution (CC BY) license (<https://creativecommons.org/licenses/by/4.0/>).

1. Introduction

Our planet is experiencing rapid climate change due to global warming, including extreme weather, changes to the seasonal weather patterns, record-breaking temperatures, and rising sea levels. Thus, global warming is a serious threat to the welfare of our planet.

Global warming is brought about by the emission of greenhouse gases (GHG), such as carbon dioxide (CO₂). The total CO₂ level in our atmosphere, which has remained relatively stable for over a millennium, has risen exponentially during recent times, increasing by more than 30% since the 1800s and exceeding the global threshold of 400 ppm in 2015 [1], while CO₂ emissions have increased by 135% since the 1970s, reaching a peak of 33.3 gigatons of CO₂ in 2019 [2]. As shown in Figure 1, the power and the transportation sector constituted almost three-fifths of the world's CO₂ emissions in 2016 [3]. Thus, reducing their dependence on fossil fuels will make a significant contribution to countries becoming carbon neutral.

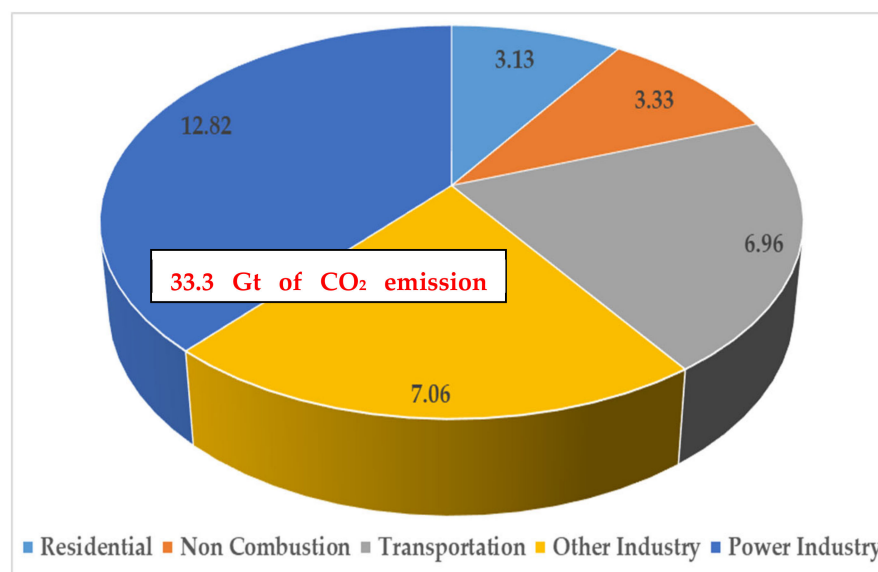


Figure 1. Breakdown of CO₂ emissions, in gigatons of CO₂, by industry sector [3].

To counteract the effects of climate change caused by the excessive release of greenhouse gases into the atmosphere, the European Union (EU) has taken the initiative to reduce its dependence on fossil fuels and become carbon neutral by 2050, as part of the European Green Deal [4]. One such initiative is the Horizon 2020, the EU research and innovation program, in collaboration with universities and industries, that aims to tackle climate change, boost the EU's global competitiveness, and achieve sustainable growth and development [5]. Thus, the purpose of the EU project, ASSURED, which is part of the EU's Horizon 2020 framework, is to boost the electrification of urban heavy duty (HD) and medium duty (MD) vehicles, such as buses and trucks, through integration with superfast charging infrastructure [6]. ASSURED also aims to develop and test high-powered interoperable solutions using innovative charging strategies (CS) for fully sized HD applications. To fulfil this goal, the research aims to investigate the total cost of ownership (TCO) of HD and MD electric vehicle fleets in cities, understand the impact of fast charging profiles on battery lifetime and sizing, and analyze the impact on the grid for a given mission profile. Furthermore, various ECO strategies, including ECO-comfort, ECO-driving, and ECO-charging are investigated to reduce the TCO and grid impact. Finally, the ability of the electric bus (E-bus) fleet, consisting of buses with different configurations, to respect the scheduling constraints set by the city bus operators (CBOs) and the constraints of the state of charge (SoC) of the energy storage systems (ESS) set by the original equipment manufacturers (OEMs), while following their daily mission scenario in a given route is evaluated through extensive use case (UC) simulations. This paper will focus on E-bus fleets and the high-power opportunity charging infrastructure necessary to allow the buses to fulfil their routine driving scenarios.

1.1. Electric Buses

According to the European Commission on Mobility and Transport, an efficient and well-planned public transport system is important in reducing the numerous traffic afflictions facing metropolitan centers, including congestion and harmful vehicular emissions [7]. Having plenty of accessible electrified public transport increases the mobility coefficient of a city's residents, thus improving business and logistics and providing health benefits. This leads to increases in the productivity and long-term financial gain of the city. One of the key aspects of electrification is the replacement of buses with internal combustion engines (ICE) with that of hybrid electric or fully E-buses. These bring numerous challenges, including investing in opportunity charging infrastructure along bus routes, electrified bus depots for overnight charging, and replacing the entire ICE-based bus fleet with buses with electric or hybrid powertrains [8]. All these challenges must be overcome to make electrified public transportation successful and financially viable. The benefits include zero-emission vehicles inside urban areas.

One of the disadvantages of electric vehicles (EVs), when compared to ICE-based vehicles, is the lack of driving range that an EV can manage, even with a fully charged ESS. To illustrate this point, let's take an example of a 12 m diesel bus, with a 227-L fuel tank, used for public transport in urban areas, and with the worst (midsummer, pre-1995 model) fuel efficiency of 80 L/100 km [9]. Even with such a dreadful fuel efficiency, the diesel-powered bus can easily cover its entire daily route of up to 250 km on a single tank of fuel; furthermore, it takes less than 10 min to refuel its tank at a filling station. In comparison, a 12 m battery electric bus (BEV) has an average energy consumption of 1.45 kWh/km [10,11]. Thus, allowing for a Depth of Discharge (DoD) of 70%, the bus would require an ESS with a capacity of 500 kWh to cover the daily transit requirement of 250 km [12]. Such a battery, depending on its chemistry, would occupy 1000 L of space, weigh 2.7 tons, and cost around €100,000 [13], which is basically a third of the capital investment for a 12 m bus. Finally, using a 600-kW ultrafast charger, it would take at least half an hour to fully recharge the ESS. Thus, to make it more feasible to deploy for CBOs, the ESS capacity will most likely be downsized to allow only one or two return trips along its route, while relying on opportunity charging at the route ends to fully charge the ESS for subsequent trips. ASSURED considers 9 m, 12 m, and 18 m articulated E-buses from different vendors, including VDL, VOLVO, IVECO, IRIZAR, and SOLARIS. However, in this paper, only 12 m and 18 m buses are considered.

1.2. Charging Infrastructure

To meet the requirements of the EU 2050 carbon neutral objective, by 2030, a 15-fold increase in public EV charging points will be required at 3 million charging points that will serve a projected 44 million EVs. Over the next decade, €20 billion in investments will be made to deploy the necessary charging infrastructure [14]. These investments will bring about an integrated ultrafast public charging network all over Europe. Electrification of the mass transit system is necessary to reduce the harmful vehicular emissions inside urban areas. Electrification of the public transport system will also reduce the overall CO₂ emissions inside the city limits, since polluting electric power plants are typically located in the outskirts of a city, whereas electricity can (and should) also be obtained from clean and renewable sources, such as wind, solar, and hydroelectricity. Thus, deploying an electrified public transportation system in cities, thereby maximizing the use of electricity from renewable sources, will allow urban residents to enjoy an improved air quality. In addition to the actual DC fast charging hardware (H/W), the charging infrastructure also depends on high voltage (HV) and medium voltage (MV) grid lines, transformer sub-stations, and ESS backup to support the ultrafast opportunity charging stations and charging depots.

For E-buses, the primary means of connection to the charging station is via the pantograph mechanism. It can either be the down pantograph, where the pantograph connection drops down from the charging station to fit into the slot in the bus, or the up

pantograph, where the pantograph connection rises from the bus to fit into the slot in the charging station. Alternatively, buses also have a plug-in charging connection based on combined charging system v2 (CCS2) connectors. The power rating of the opportunity chargers can range from the fast 290 kW to the ultrafast 600 kW charger, will be DC, and will mainly use the pantograph system, while overnight charging in the depot can either be AC or DC, with a power rating ranging from 50 kW to 150 kW, and utilize either pantograph or plug-in charging systems.

1.3. Goals and Objectives of the Paper

The purpose of this paper is to demonstrate the use of simulations for optimizing the operation of E-bus fleets. A simulation platform, including an energy consumption and cost evaluation of the entire fleet, is utilized to obtain a detailed overview of the operation. Different energy management strategies are evaluated in the simulation platform, and multi-objective optimization algorithms are utilized to find the most suitable strategy in terms of both costs and environmental impact.

The paper is outlined as follows. In Section 2, the simulation framework is presented, including both the technical description and the cost evaluations. The details of the studied UCs, i.e., the routes, vehicles, and operational scenarios are outlined in Section 3. The different ECO features regarding energy and charging management that can be applied within the simulation are presented in Section 4, and the optimization techniques are provided in Section 5. Finally, the results and the conclusions are given in Sections 6 and 7, respectively.

2. Description of the Simulation Framework

In ASSURED, a low-fidelity (Lo-Fi) simulation framework has been developed that will allow the user to evaluate the energy expenditure for fleets of vehicles, the daily impact on the grid, and the TCO for a given mission profile. The Lo-Fi models are based on basic electrical, mechanical, kinematic, and thermal equations to represent the transformer, the charger, and the forward-facing E-bus powertrain model, as shown in Figure 2. The Lo-Fi model uses Look-up Tables (LuTs) to model the efficiency maps of the transformer, the charger, the DC-DC converter, and the inverter and electric machine combination. The output of the LuT can be a function of one or more inputs, as shown in Table 1. The ESS models are complex and require several LuTs to describe the open circuit voltage (OCV), the relative capacity degradation (RCD), the series (R_s) and polarization resistance (R_p), and the time constant (T_c) of the modeled capacitors. The efficiency map of the transformer is generated from a high-fidelity (Hi-Fi) simulation of a generic transformer in MATLAB/Simulink. The efficiency map of the charger is constructed from data supplied by the charger OEM, while its power factor (PF) map (which outputs the PF experienced by the grid during charging) is created from a Hi-Fi simulation of a generic charger in MATLAB/Simulink. The efficiency map of the DC-DC converter is derived from a Hi-Fi simulation of a SiC-based interleaved bidirectional converter [15] in MATLAB/Simulink. The efficiency map of the inverter and electric machine has been created from experimental tests. The maps for the ESS have been generated from experimental tests. These maps ensure a measure of realism by ensuring dynamic changes due to changing conditions, without sacrificing speed. The simulation framework uses the Lo-Fi model based on LuTs, instead of a Hi-Fi model, to ensure that large fleets of E-buses can be simulated within a reasonable timeframe.

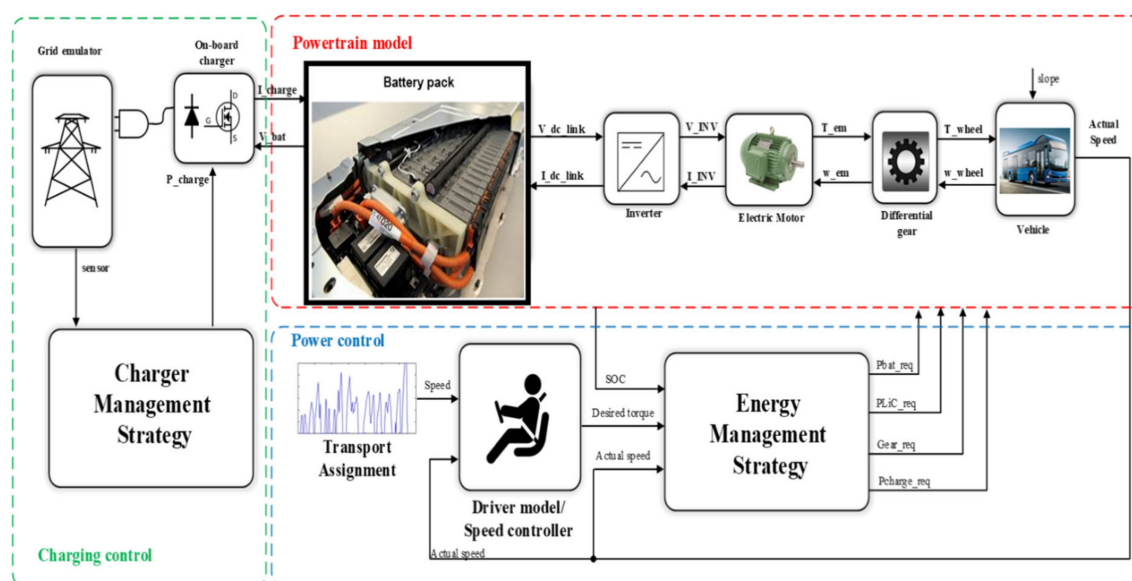


Figure 2. Forward-facing model of the electric vehicle powertrain.

Table 1. List of the LuTs used in the simulation framework.

Component	Type of LuT	Dependency
Transformer	Efficiency map	Load (VA) PF (-)
Off board charger	Efficiency map	Load (kW) Output voltage (V)
	PF map	Load (kW)
Main DC-DC converter	Efficiency map	Output voltage (V) Output current (A)
Auxiliary DC-DC converter	Efficiency map	Load (kW)
Electric machine and inverter	Efficiency map	Angular speed (rad/s) Output torque (Nm)
	Torque-speed map	Angular speed (rad/s)
Energy storage system	OCV map	SoC (%) Temperature (°C)
	RCD map	Charging rate (C) Equivalent charge/discharge cycles (-) Temperature (°C)
	Series resistance map	Charging rate (C) SoC (%) Temperature (°C)
	Polarization resistance map	Charging rate (C) SoC (%) Temperature (°C)
	Time constant	Charging rate (C) SoC (%)
		Temperature (°C)

The inputs of the simulation framework include the driving (speed) profile, the charging profile, the passenger load profile, the weather profile (temperature, humidity, solar irradiance, wind, rainfall, and cloud coverage), and the road elevation profile. The driving scenario uses the hybrid SORT profile, which is adapted to the average driving

speed of the route. The charging profile (charging rate) depends on the battery chemistry and charger power rating and uses the constant-current and constant voltage (CC/CV) mode of charging. The passenger load profile is entirely randomized throughout the simulation but has an upper limit based on the bus size and resetting to zero every time the bus reaches the end of a route. The elevation profile is specific to the route and provided by the CBO. Finally, the weather profile is dependent on the city being simulated and is based on historical average monthly climate data for that city [16]; these have been acquired from publicly available meteorological data. The cities of Barcelona, Gothenburg, Jaworzno, and Osnabruck are participating in the ASSURED project; however, Table 2 only lists the weather data for the two cities considered in this paper.

Table 2. Climate data of the cities [16].

City		Month											
		JAN	FEB	MAR	APR	MAY	JUN	JUL	AUG	SEP	OCT	NOV	DEC
Barcelona	Hi (°C)	15	15	17	20	23	27	29	29	26	23	18	15
	Lo (°C)	9	8	10	13	16	20	23	23	20	17	12	9
	Hum (%)	69	66	73	69	68	67	67	72	74	74	72	70
	Day (h)	9.5	10.5	12	13.5	14.5	15	15	14	12.5	11	10	9.5
	Sun (%)	87	86	84	80	87	90	97	94	87	81	83	90
Gothenburg	Hi (°C)	2	3	6	11	17	20	22	21	17	12	7	4
	Lo (°C)	−2	−2	0	3	8	12	14	13	10	6	2	0
	Hum (%)	85	82	77	71	66	69	73	74	79	81	86	86
	Day (h)	7.5	9.5	11.5	14.5	16.5	18	17.5	15.5	13	10.5	8	7
	Sun (%)	68	71	74	73	74	73	71	68	67	65	60	62

The simulation framework can also be configured via a user interface to tune it for different UCs. The interface of the E-Bus allows the bus to be tuned to different bus sizes, battery sizes and chemistries, cities and routes, and driving and charging scenarios. The mission specific details of the UCs will be described in the next section. The climate data from Table 2 are utilized in the simulation framework for all the cities participating in the ASSURED project, with the daily variation between the high and low temperatures and variation in the solar irradiance introduced. The road elevation, bus frequency, average driving speed, operational time of the bus, and the charging type and duration can also be defined for a route. All this information is utilized by the simulation framework to evaluate the energy requirement of the bus and the impact on the local grid. The aim of the simulation framework is not to conduct detailed simulations of every parameter and situation, but to keep track of the overall energy flow within the system as the E-Bus follows a typical mission scenario. The simulation framework has been made scalable to handle fleets of E-buses and multiple bus routes in a city. The transformer design allows it to interact with multiple chargers of varying power ratings simultaneously. Similarly, each charger can interact with a fleet of E-buses according to their charging schedules, and each E-bus can interact with chargers in different locations. The E-buses make use of bus IDs to differentiate themselves from each other to a charger.

2.1. Electric Bus Powertrain

The following equations govern the behavior of the power relations in the backward dynamics of the EV powertrain model shown in Figure 2. We start with the overall tractive force (F_T) that needs to be provided to cause the required acceleration of the vehicle represented in Figure 3.

$$F_T = m \times g \times (F_R \cdot \cos\alpha + \sin\alpha) + \frac{1}{2} \rho \times C_D \times A \times (v + V_W)^2 + (m + M_F) \times dv/dt \quad (1)$$

where m is the vehicle mass (kg), g is the gravitational acceleration (9.81 m/s^2), F_R is the rolling resistance coefficient, α is the road gradient angle (rad), ρ is the air density (1.226 kg/m^3), C_D is the drag coefficient, A is the vehicle frontal cross sectional area, v is the vehicle speed (m/s), V_W is the frontal windspeed (m/s), M_F is the mass of rotational inertia (kg), and dv/dt is the vehicle acceleration (m/s^2). The total force required to propel the vehicle forward has five components, namely, the rolling resistance (cos), the grade resistance (sin), the aerodynamic drag, the inertial resistance, and finally, the accelerating force. The set of Lo-Fi equations for individual components of the electric bus powertrain are given in the Appendix A.

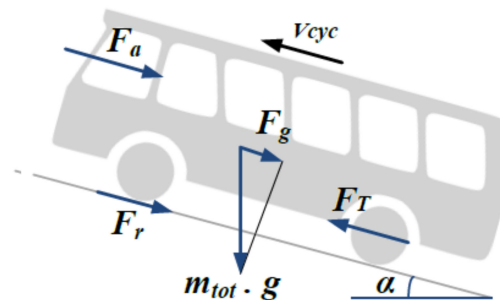


Figure 3. The forces acting on a vehicle in motion.

2.2. Charging Model

The DC charger is composed of two stages, a step-down transformer and rectifier stage, followed by a DC-DC converter stage. Since the backward dynamics are being described, the DC-DC converter stage will be presented first, followed by the transformer and rectifier stage. The equations are given in the Appendix A. The equations for the charging infrastructure consider multiple chargers that will be consuming electricity from the substation transformer.

2.3. Total Cost of Ownership

A TCO analysis of a bus fleet must always be made on a system level to include all the relevant costs. As a first step, the productivity of the bus fleet must be confirmed, i.e., that the buses are able to fulfil the required duty cycles without failure. In the second step, the total cost of the operation can be evaluated. The total cost of ownership of an electric bus fleet consists of the capital expenses as well as the operational expenses. The capital costs arise from owning a bus fleet, i.e., purchasing the vehicles and the required charging infrastructure, while the operational costs arise from the energy, service, and maintenance, as well as salary costs.

In the evaluation of the capital costs, the service life of each component is an important parameter. In this paper, the electric buses and charging infrastructures are assumed to last for up to 15 years under standard operating conditions. An exception to this is the lifetime of ESS, which is assumed to have a lifetime of 8 years and will thus need to be replaced at least once during the lifetime of the bus. The battery is also one of the most expensive parts of an electric vehicle, and its lifetime is highly dependent on the usage of the bus. Hence, accurate battery modelling, sizing, as well as a detailed model of the operation and energy consumption, are crucial to obtain a realistic view of the battery investment costs. However, uncertainty related to future battery prices and battery characteristics remain. Battery prices are generally forecasted to decrease in the coming years. Under this assumption, the battery can be replaced by a new one with a similar capacity but at a lower price, or it can be replaced by a battery with the same price as the initial one but with a higher energy and/or power capacity. In the first case, the operation of the electric bus will continue as it did previously, but the capital costs related to the battery replacement will be lower than what could be expected based on today's price levels. In the other case, the operation of the bus can potentially be improved, as the amount and/or duration of charging can be

reduced. However, the battery prices in the heavy-duty vehicle segment may not decrease in the same manner as in the light vehicle segment, where mass production quantities are higher, thus lowering the price levels as light EVs become more common.

When it comes to the charging infrastructure, the utilization of the charger is important. A thorough analysis of the operation of the bus fleet provides information on how many chargers are required for serving the fleet. As the lifetime of a charger is long, future upscaling of the electric bus fleet can have an impact on the costs related to the charger investments. For instance, locating a charger where multiple buses and bus lines can utilize the same infrastructure can reduce the overall TCO in the long run, even though the infrastructure is oversized during the very first years of operation. In the simulation platform, the costs are evaluated individually for each vehicle, and the total costs are obtained as a sum of these costs. The TCO can be expressed as the sum of the capital costs and the operational costs:

$$TCO = TCO_{CAP} + TCO_{OP} \quad (2)$$

where TCO_{CAP} and TCO_{OP} denote the total capital costs and the operational costs, respectively. The capital costs can be expressed as:

$$TCO_{CAP} = TCO_{VEH} + TCO_{BAT} + TCO_{CHAR} \quad (3)$$

where 'VEH' represents the vehicle, 'BAT' represents the ESS, and 'CHAR' represents the charger. The vehicle capital expense (per km), TCO_{VEH} , is calculated as:

$$TCO_{VEH} = C_{VEH} / (L_{VEH} \times D_{YEAR}) \quad (4)$$

where C_{VEH} is the purchase price of the vehicle, L_{VEH} the estimated vehicle lifetime, and D_{YEAR} is the estimated yearly mileage. The D_{YEAR} for all routes is assumed to be 45,000 km/year; under this assumption of the yearly mileage travelled, the L_{VEH} is assumed to be 15 years. The battery expense, TCO_{BAT} is calculated as:

$$TCO_{BAT} = C_{BAT} / (L_{BAT} \times D_{YEAR}) \quad (5)$$

where C_{BAT} is the purchase price of the battery, L_{BAT} is the estimated battery lifetime, and D_{YEAR} is the estimated yearly mileage of the vehicle. L_{BAT} depends on the usage of the battery, as explained above; however, under the assumption that D_{YEAR} is 45,000 km/year, L_{BAT} is assumed to be 8 years for all batteries, except for LTO batteries, which are assumed to have a lifetime of 15 years. The charger expense is calculated as:

$$TCO_{CHAR} = (\sum C_{CHAR}) / (L_{CHAR} \times D_{YEAR} \times N_{VEH}) \quad (6)$$

where C_{CHAR} is the purchase price, the installation cost, and the grid connection cost of all the chargers, L_{CHAR} is the estimated charger lifetime, D_{YEAR} is the estimated yearly mileage of the vehicle, and N_{VEH} is the number of vehicles sharing the same charger. It is assumed that all chargers have similar lifetimes of 15 years; in reality, they would vary depending on the manufacturer, power rating, and operational conditions, such as frequency or intensity of use and the average and peak power load on the charger. The operational cost is calculated as:

$$C_{OP} = \frac{C_{EL} \left(\int_{t=0}^{t=t_{END}} P dt + (SOC(t_{END}) - SOC(0)) \times E_{ESS} \right) + C_{EX} \times (P_{MEAN} - P_{CUT})}{\int_{t=0}^{t=t_{END}} v dt} \quad (7)$$

where C_{EL} is the electricity tariff, P is the charging power, SoC is the state of charge of the battery, and C_{EX} is the excess power usage surcharge applied when $P_{MEAN} > P_{CUT}$, where P_{MEAN} is the maximum hourly running average power consumption, and P_{CUT} is the threshold, beyond which the power usage is in excess. C_{EL} is taken to be 0.1 €/kWh in Barcelona and 0.05 €/kWh in Gothenburg [17]. C_{EX} is assumed to be 0.1 €/kW, and

P_{CUT} is assumed to be 10 kW. For simplicity, the service and maintenance costs are omitted from the analysis. The salary costs are also omitted, which means that the operational costs consist of only the energy-related costs. The installation costs of the chargers [18], used in the UCs simulations for single and fleets of e-buses, have been taken from a detailed survey conducted of the charging infrastructure in multiple metropolitan cities. The capital costs of the ESS [19] are taken from literature, while the vehicle and charger costs are supplied by the OEMs.

The total costs of the chargers are separately considered based on their rated power, installation costs, and grid connection costs. The costs related to the charger, presented in Tables 3 and 4, is based on interpolation and extrapolation of the data provided in [18] using the spline method and then subject to a 2% inflation over a 5 year period. The grid connection charge is assumed to be 100 €/kW/year.

Table 3. Capital costs of equipment [18,19].

C_{BAT}	C_{VEH}	C_{CHAR}
NMC: 420 €/kWh	12 m bus: €300 k	100 kW: €48,273
LFP: 580 €/kWh	18 m bus: €450 k	150 kW: €68,472
LTO: 1005 €/kWh		290 kW: €113,615
		450 kW: €144,613
		600 kW: €153,721

Table 4. Installation costs of fast chargers [18].

Charger/Site	100 kW Charger	150 kW Charger	290 kW Charger	450 kW Charger	600 kW Charger
1	€42,064	€43,622	€53,510	€74,783	€104,387
2	€33,269	€34,375	€42,349	€60,267	€85,594
3–5	€24,925	€25,848	€31,706	€44,309	€61,847
6 and above	€22,035	€16,960	€20,804	€29,074	€40,582

3. Details of the City Routes and Vehicle Types

This section provides a brief overview of the cities and the routes, as well as the electric buses that will be simulated in the simulation framework. The paper is an extension of the research carried out in [15,20]; however, this paper considers two cities with completely different climates to each other, four different E-bus models as part of a fleet, and multiple routes with different characteristics. The effect of all this variability on the vehicle energy requirements is investigated. The seasonal effects (i.e., summer and winter) and the effects of ECO features on the energy requirements are also investigated and are presented in subsequent sections.

3.1. City of Barcelona

Barcelona, Spain has a Mediterranean climate, with hot and humid summers and mild winters. Most of the rainfall occurs during the winter months. Table 2 presents the annual climate details for the city, while Figure 4 gives a daily snapshot of the weather for four seasons, which will be assumed during simulations of the city. UCs from two routes in Barcelona will be presented, the L33 and the H16 route, as shown in the map in Figure 5. Table 5 lists the configuration and mission constraints of the route and the chargers that must be factored in during the simulations. The results for a single bus, fleets consisting of four types of buses, and multi-objective optimization of the fleets will be presented for Barcelona.

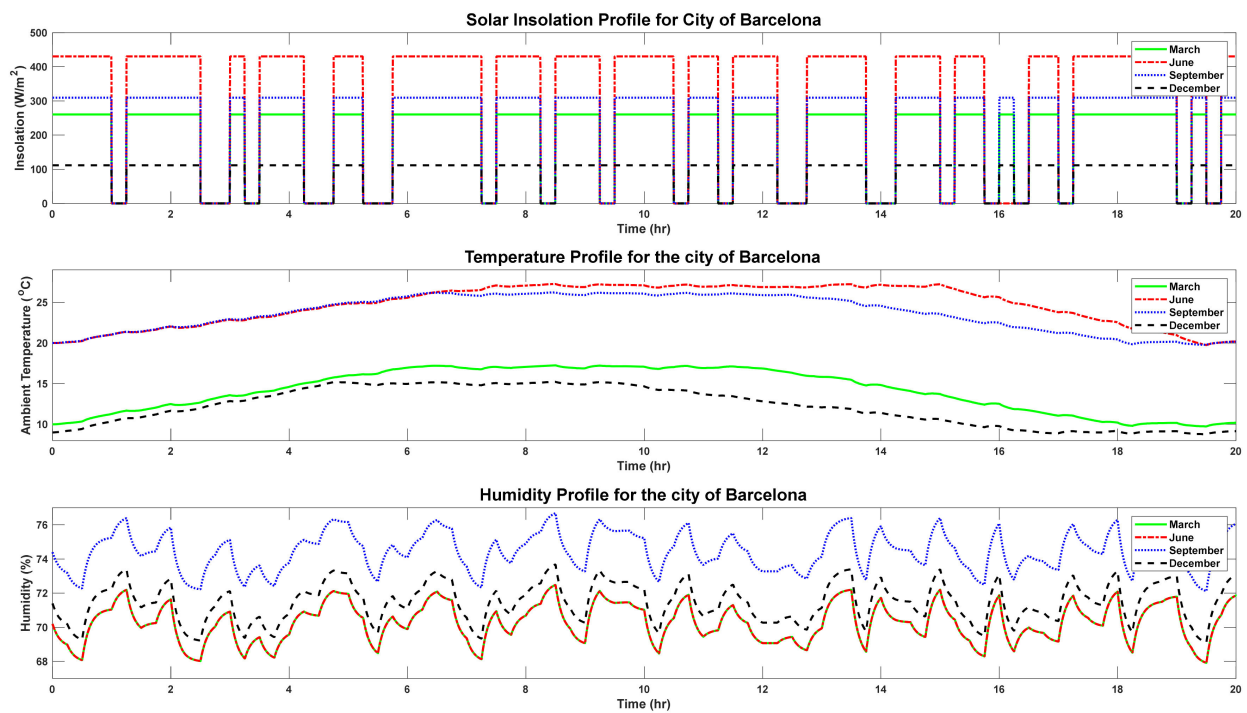


Figure 4. Seasonal climate of the city of Barcelona.

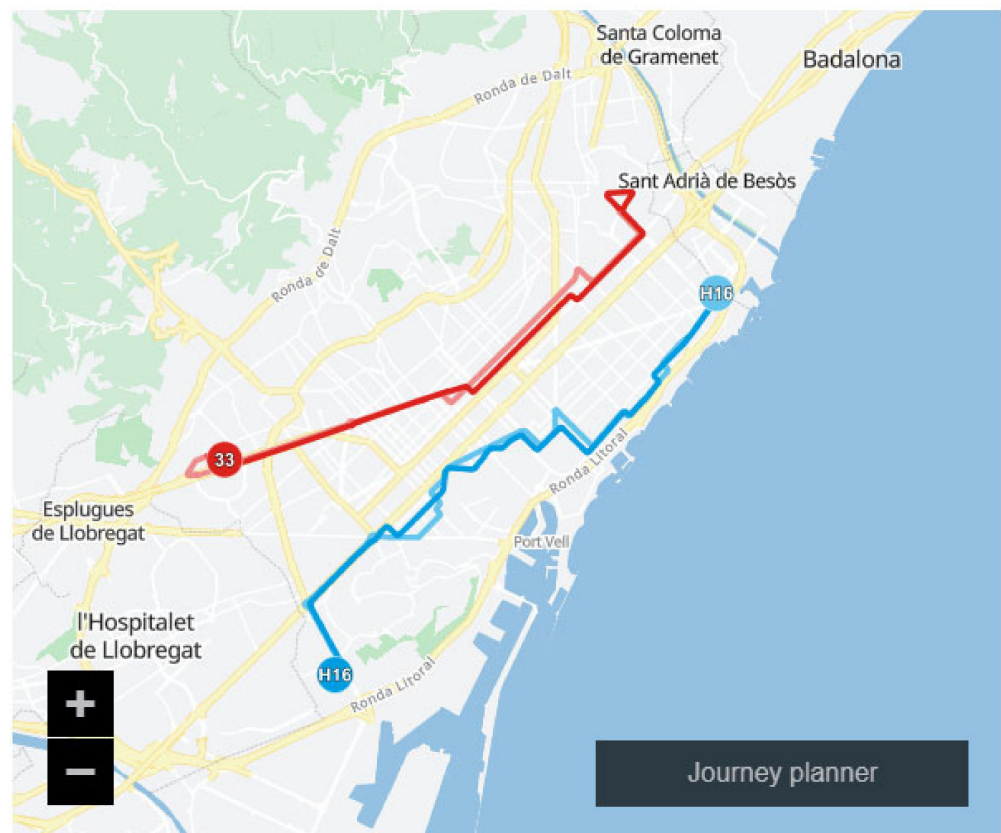


Figure 5. The map of Barcelona city, showing routes H16 and L33 [21].

Route L33 runs between Zona Universitaria and Verneda; it has a route length of 9.7 km; and a return trip takes approximately 100 min. Route H16 runs between Zona Franca and Campus Besos; it has a route length of 11.9 km; and a return trip takes approximately 2.5 h. Both routes feature the 600-kW ultrafast charger from Heliox. Figure 6 shows the elevation and velocity profile of the two routes for one return trip, which are inputted into the simulation platform. Figure 7 shows the daily passenger profile considered for the two routes for both the 12 m and 18 m bus types. The profile shown in Figure 7 is only shown for the first bus in the fleet; subsequent buses in the fleet will have these shifted in time, according to their schedule. Furthermore, since the passenger load profile is completely randomized, the actual passenger trend in the different schedules will differ slightly from the plot shown and from each other. However, the daily passenger profile for a given bus is assumed to remain the same for all days of the entire year. This similarity in the passenger profile will allow for a comparison to be made between seasons.

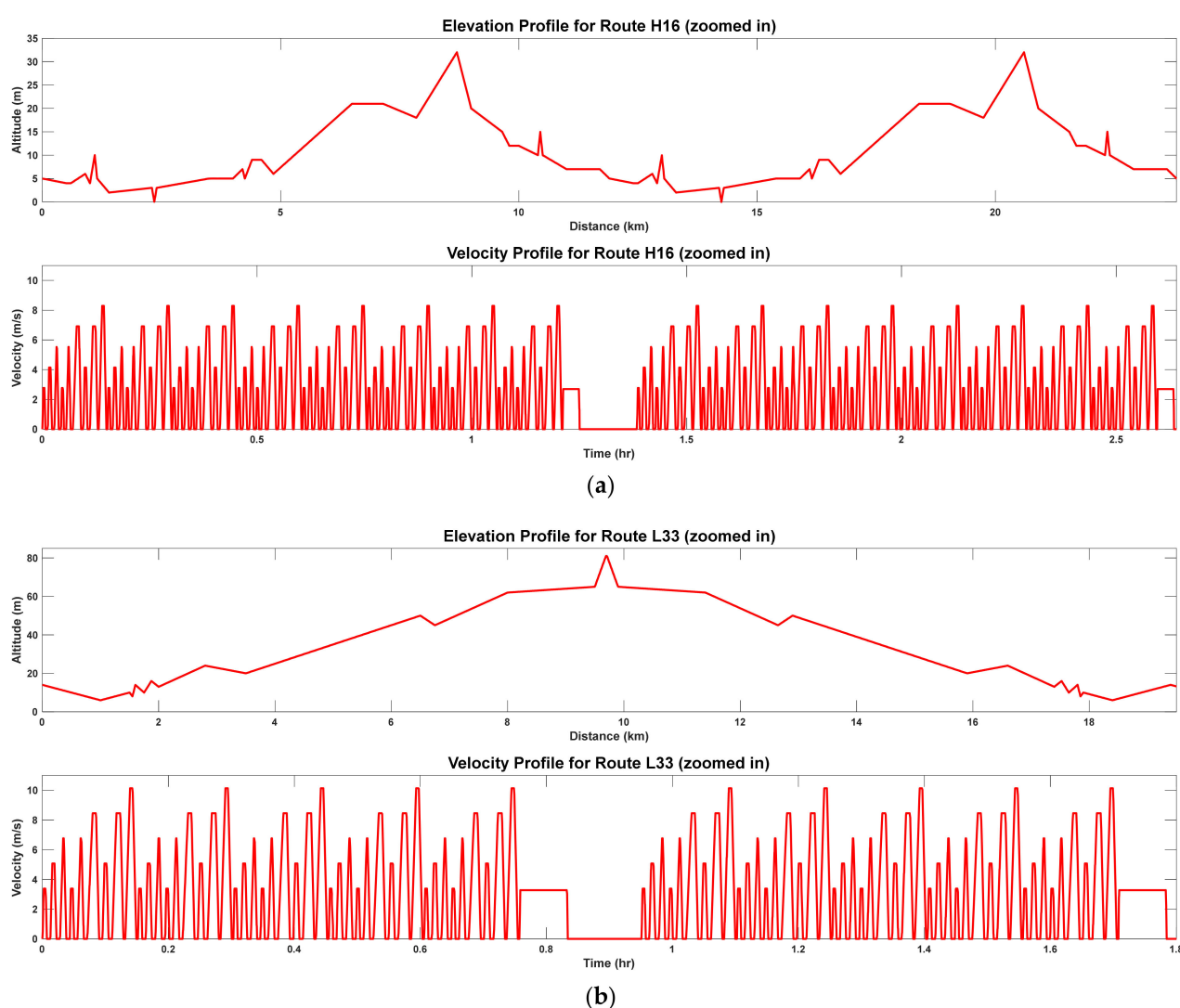


Figure 6. The route elevation and velocity profiles for one return trip for (a) Route H16 and (b) Route L33.

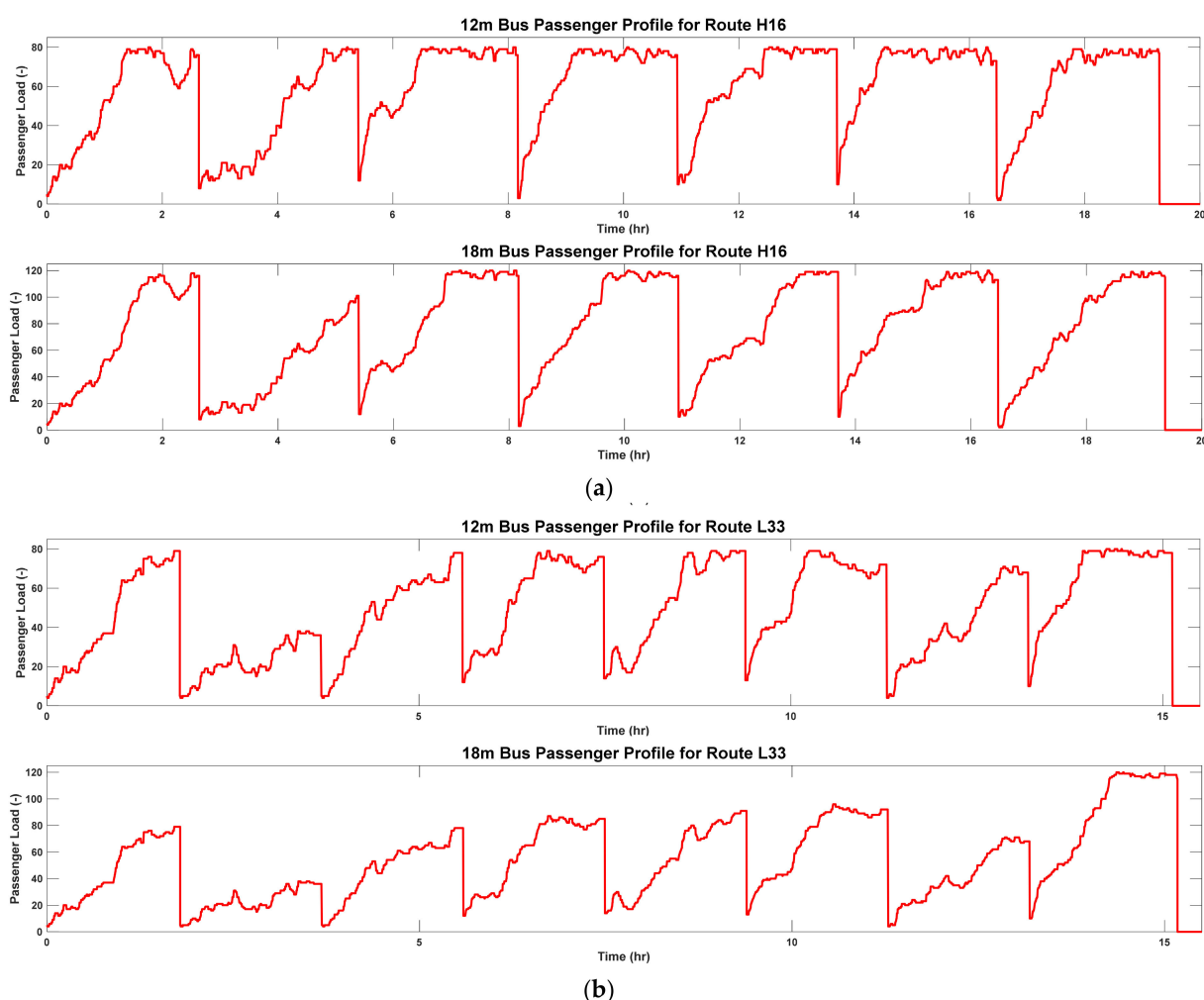


Figure 7. The daily passenger profiles shown for 12 m and 18 m buses on (a) Route H16 and (b) Route L33.

Table 5. Scenario details of the routes in Barcelona city.

Parameters	Route 1	Route 2
Route	L33	H16
Max. acceleration on flat ground (m/s ²)	1.5	1.5
Operational time per day (h, kms)	15.33 h, 155 km	17.33 h, 165 km
Bus frequency (peak hours)	Every 7 min	Every 8 min
Number of stops per bus line	27	35
Average speed of the bus during peak hour (km/h)	11.64	9.52
Return trip distance (km)	19.4	23.8
Number of return trips per day	8	7
Total number of buses in route (-)	16	20
Type of buses in route T	4 × each type	5 × each type
Ambient temperature (°C)	Min: 8 °C, Max: 29 °C	
Charger		
Charging Scenario	Opportunity, AC/DC, CCS 2	
Max. Number of Intermediate Charging Instances per Cycle	1	
Max. Charging Power for On-road Superfast Charging (kW)	600	
Available Superfast Charging at Terminals or Stops (mins)	3–8	
Power Charging for Overnight Stations (kW)	100	
Overnight Charging Time Available (h)	2–5	
Grid Capacity (kVA)	300–600	
Cost of Connection of Charger to Grid (€/charger)	200,000	
Lifetime of Charger (years)	15	

3.2. City of Gothenburg

Gothenburg, Sweden has an ocean climate, according to the Köppen climate classification [22], with mild summers and cold winters. The city experiences plenty of rainfall throughout the year. Being a coastal city, the diurnal temperature variations are moderate. Table 2 presents the annual climate details for the city, while Figure 8 gives a daily snapshot of the weather for four seasons, which will be assumed during the simulations for the city.

For the single bus simulations, the UCs from route R55 in Gothenburg will be presented, while for the fleet and multi-objective optimization, routes R55 and EL16 will be considered. Figure 9 shows the two routes, while Table 6 lists the configuration and mission constraints of the route and the chargers that must be factored in during the simulations. In Gothenburg, all buses are of the same type.

Route EL16 runs between Eriksbergstorget and Sahlgrenska Sjukhuset; it has a route length of 11 km; and a return trip takes approximately 56 min. Route R55 is a subset of route EL16; it runs between Teknikgatan and Sven Hultin Plaats; it has a route length of 7.6 km; and a return trip takes approximately 50 min. Another difference between EL16 and R55 is in the charging system used. While both routes are essentially the same, the buses traveling along the longer EL16 route will be charged using the 450 kW ABB superfast charger, while the buses traveling along the shorter R55 route will be charged using the Siemens 290 kW fast charger. A final difference is in the speed of the vehicle. The buses traveling on route EL16 travel on average more than 5 km/h faster than the buses traveling on route R55. As a note, although the buses on route EL16 will be charged using the 450-kW charger, the bus itself will limit itself to 290 kW; thus, the charger will only be loaded by two-thirds. On the other hand, the 290-kW charger on route R55 will be fully loaded during charging.

Figure 10 shows the mission scenario, consisting of the elevation, velocity, and passenger profiles of the two routes, which are inputted into the simulation platform. The elevation and velocity profile are shown for one return trip, while the passenger profile is shown for the whole day. The same assumptions regarding the passenger profile as those given for Barcelona are also applied in Gothenburg.

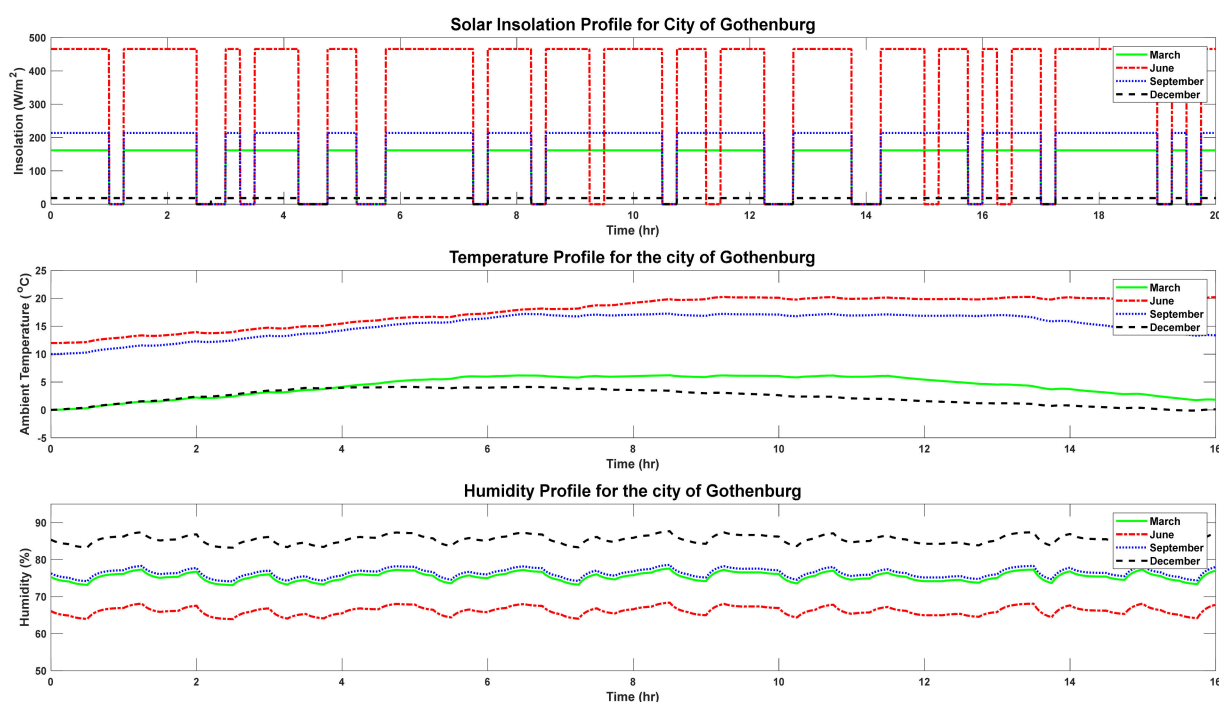


Figure 8. Seasonal climate of the city of Gothenburg.

Table 6. Scenario details of the routes in Gothenburg city.

Parameters	Route 1	Route 2
Route	R55	EL16
Max. acceleration on flat ground (m/s ²)	1.5	1.5
Operational time per day (h, kms)	13 h, 167 km	20 h, 396 km
Bus frequency (peak hours)	Every 10 min	Every 5 min
Number of stops per bus line	13	22
Average speed of the bus during peak hour (km/h)	18.24	23.57
Return trip distance (km)	15.2	22
Number of return trips per day	11	18
Total number of buses in route (-)	7	13
Type of buses in route 7	All the buses are of type 2	
Ambient temperature (°C)	Min: −2, Max: 22	
Charger		
Charging Scenario	Opp, AC/DC CCS2	Opp, AC/DC CCS2
Max. Number of Intermediate Charging Instances per Cycle	2	2
Max. Charging Power for On-road Superfast Charging (kW)	290	450
Available Superfast Charging at Terminals or Stops (mins)	8–10	4–5
Power Charging for Overnight Stations (kW)	150	150
Available Overnight Charging Time (h)	1–10	1–10
Grid Capacity (kVA)	>350	>350
Cost of Connection of Charger to Grid (€/charger)	200,000	200,000
Lifetime of Charger (years)	15	15

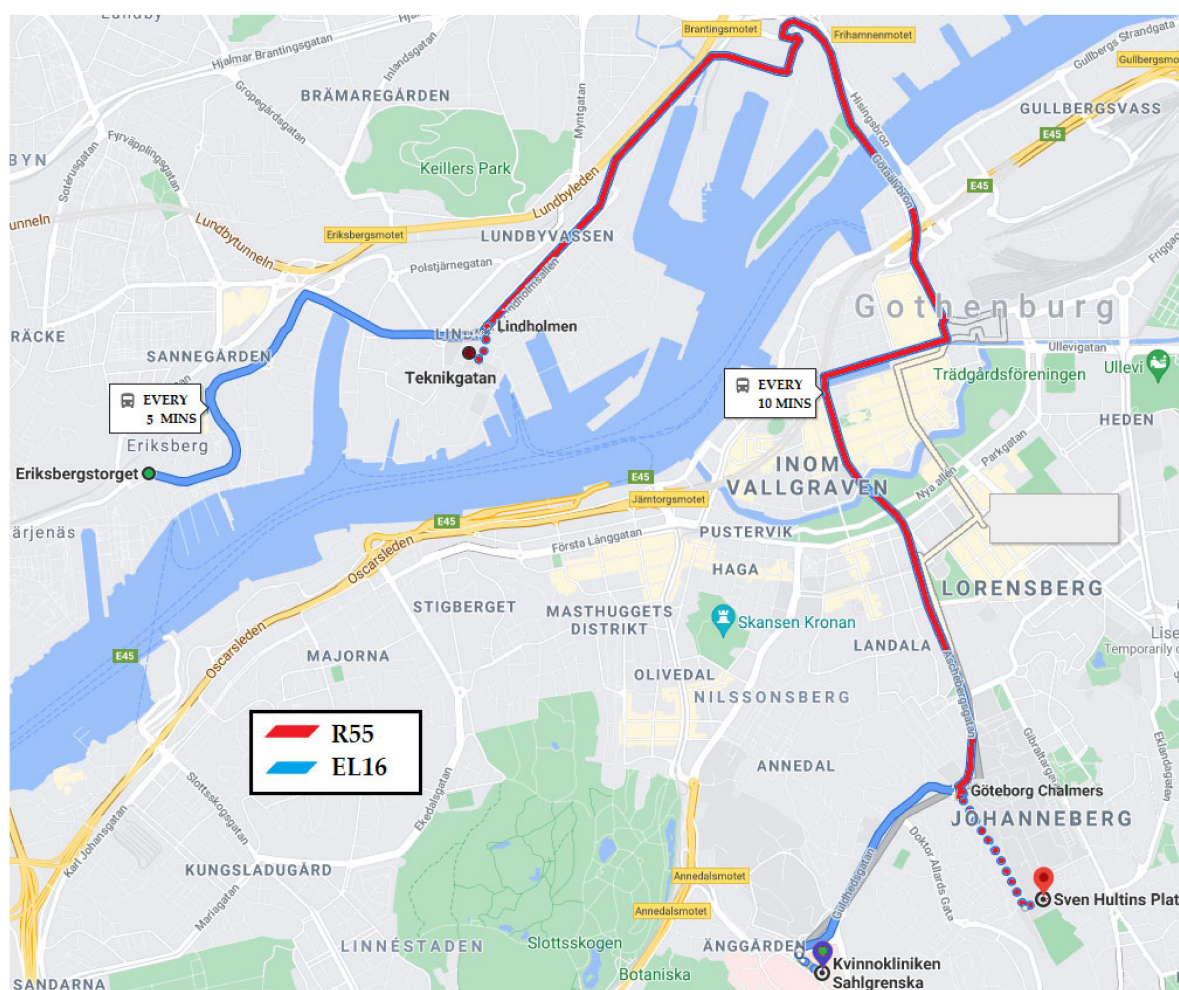
**Figure 9.** The map of Gothenburg city, showing routes R55 and EL16 [23,24].



Figure 10. The road elevation, velocity, and passenger profiles for routes (a) R55 and (b) EL16.

3.3. Types of E-Buses in the Fleet

This section gives an overview of the E-buses that were considered in the simulation. Four types of buses were considered: two 18 m buses and two 12 m buses. The 18 m buses use lithium titanate (LTO) batteries as their ESS, while the 12 m buses use lithium ferro-phosphate (LFP) and lithium nickel-manganese-cobalt (NMC) batteries. Furthermore, for the 18 m buses, compared to the size of the bus, the capacity of the ESS is in the low end and will barely allow two return trips, while the 12 m buses have the capacity to allow for

multiple return trips. On the other hand, the LTO battery chemistry of the ESS in the 18 m buses allow for superfast charging using high-powered chargers. These factors need to be considered by the charging management system (CMS) to ensure that the SoC do not fall below the OEM specified constraints. Table 7 lists the specifications of the different types of buses that are considered for simulation.

Table 7. Types of buses and their unique specifications considered for the fleet simulation.

Parameters	Type I	Type II	Type III	Type IV
Vehicle				
Dimensions (m)	$17.97 \times 3.35 \times 2.55$	$12 \times 3.3 \times 2.55$	$18.73 \times 3.4 \times 2.55$	$12 \times 3.51 \times 2.55$
Empty mass (t)	19	11.9	18.7	12.9
Maximum mass (t)	30	19	28	19.1
Gearbox				
Final gear ratio	5:75	5:77	1:6	1:4
Gear efficiency (%)	92	97	95	96
Electric Machine				
Motor type	Induction	Permanent magnet	AC synchronous	Permanent magnet
Cont. power (kW)	170	185	235	153
Base speed (rpm)	4075	4200	1000	600
Max. torque (Nm)	400	425	2300	2500
Efficiency (%)	LuT	LuT	LuT	LuT
Max. DC Link (V)	780	660	700	690
Min. DC Link (V)	520	420	700	470
ESS				
Cell technology	LTO	LFP	LTO	NMC
Capacity (Ah)	160	336	180	300
Max. SoC (%)	100	90	100	90
Min. SoC (%)	15	10	15	10
Usable energy (kWh)	90	160	108	138
Max. Voltage (V)	780	768	700	680
Min. Voltage (V)	520	422	700	470
Max. charge rate	5C	3.75C	5C	2.5C
Max. discharge rate	10C	7.5C	10C	5C
Lifetime (years)	15	8	15	8
Mass (kg)	1340	1440	1575	1980
Auxiliary				
Voltage (V)	24	600	24	24
Power (kW)	25	28	44 (heat), 39 (cool)	25
Operational				
Max. speed (km/h)	50	80	50	40
Annual distance (km)	45,000	45,000	45,000	45,000
Vehicle lifetime (years)	15	15	15	15

4. ECO Features

This section elaborates on the various economy or “ECO” features and their role in reducing the energy consumption of the vehicle, the TCO of the fleet, and the load on the grid. The ECO features are energy-saving techniques that can be implemented in a vehicle’s energy management, thermal management, and charging management systems to lower the energy utilization rate, given in kWh/km, when the vehicle is in operation. This would not only lead to an increase in the electric driving range of the vehicle, but also lead to a reduction in the lifetime TCO of the vehicle. ECO features usually decrease the performance of the vehicle in certain aspects, e.g., using less responsive acceleration to decrease overall energy requirements. Three ECO features are implemented in ASSURED, namely, ECO-comfort, ECO-driving, and ECO-charging. These ECO features are described in more detail in the following subsections.

4.1. ECO-Comfort

ECO-comfort is a functionality that is developed to provide energy savings by optimizing the thermal system of the electric vehicles. It is based on the principle of providing the least amount of comfort to the maximum number of passengers, as expressed in terms of the predicted mean vote (PMV) and predicted percentage dissatisfied (PPD), in an attempt to minimize the power consumption of the HVAC system [25]. The PPD versus PMV chart, shown in Figure 11, predicts the average value that a group of people would rate their comfort level at a given ambient condition. A value of -3 indicates a “very cold” sensation, $+3$ indicates a “very hot” sensation, and 0 indicates a “neutral” sensation. For this range of sensations, the PPD will describe the percentage of people, on average, that will be dissatisfied. Because the chart deals with people’s perceptions, which are subjective, it is impossible to obtain a PPD of 0% , even when the ambient conditions are ideal. This indicates that it is impossible to satisfy everyone. Furthermore, the chart shows that people, on average, are initially resistant to feelings of discomfort under deteriorating conditions. Thus, a PMV increase by 0.5 from 0 only increases the PPD by 5% , while a similar PMV increase from 0.5 will increase the PPD by almost 25% . Thus, this allows ECO-comfort algorithms a wide range of cabin conditions that can be set to derive the maximum energy savings.

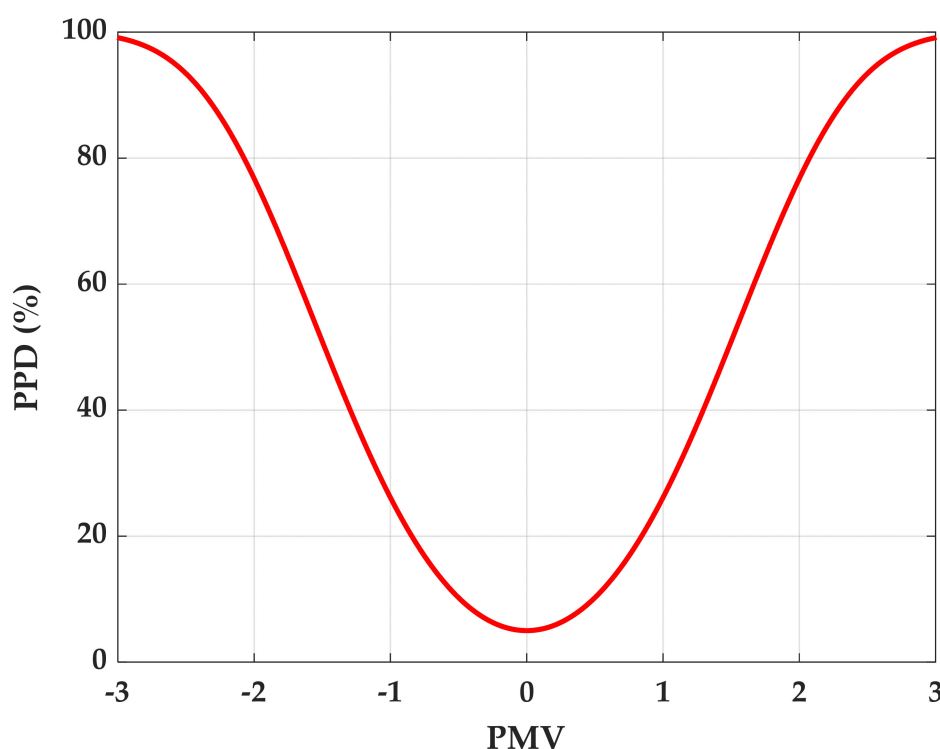


Figure 11. Relation between the Predicted Mean Vote and Predicted Percentage Dissatisfied [25].

The ECO-comfort functionality that is defined in this project has the following aspects:

- A variable temperature setpoint that considers the energy consumption of the HVAC system and the comfort of the passengers. Instead of having one fixed setting of the temperature inside the bus, a variable setting can save energy required for conditioning the air inside the bus. Three settings are defined, as shown in Figure 12:
 - A lower comfortable temperature bound that defines the lowest temperature that will be bearable to the passengers in the bus. This setting is mostly applied during winter conditions with respect to energy consumption.

- An upper comfortable temperature bound that defines the highest temperature that will be bearable to the passengers. This setting is mostly applied during summer conditions with respect to energy consumption.
 - The ideal temperature for comfort. This setting defines the temperature at which the comfort of a group of passengers is at its highest level.
- Variable air refresh rate: Depending on the temperature and humidity difference between the ambient conditions and the desired conditions inside the bus, it can require a large amount of energy to condition the air that is flowing into the bus from outside. Therefore, energy can be saved if the air inside the bus is recirculated, instead of taken from the outside. The functionality that is implemented in ECO-comfort is to optimize this fresh air flow, depending on the number of passengers that are inside the bus, instead of having one fixed value to cover most of the use conditions.
- Like the air refresh rate, the fan power can be adjusted to the number of passengers inside the bus. If there are fewer passengers inside the bus, the fan power and the corresponding air flow do not need to be at the maximum value. This will save energy that is required by the ventilation system.
- Vehicle preconditioning: The aim is to use the HVAC system to its full capacity only when the bus is connected to the charger, so the HVAC system draws the power from the charger, instead of its ESS. With preconditioning, the HVAC system will track the desired setpoint temperature, which is highly energy intensive, when the bus is charging. When the bus is not connected to the charger, the HVAC system will merely regulate the temperature around the desired setpoint, which requires minimal energy expenditure. With preconditioning, the capacity of ESS can be mostly directed toward increasing the distance that the vehicle can travel on a single charge.

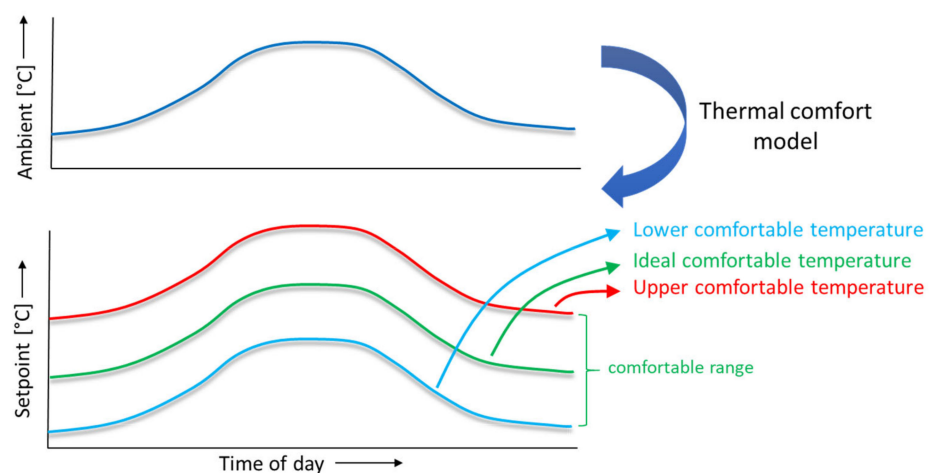


Figure 12. ECO-comfort temperature settings.

The comfort of the passengers, mentioned above, depends on many parameters, such as air humidity, air velocity, radiation, seasonal effects, and human metabolism. The combination of these factors does not have the same effect on all people's comfort, as different people will experience the same environment differently. Therefore, it is not possible to configure the cabin environment such that it will make all passengers feel comfortable; thus, the goal is to keep most of the passengers satisfied. This allows the ECO-comfort algorithm a hard PMV limit of ± 1.5 , within which to deploy energy-saving techniques. ECO-comfort has been studied in greater detail in [16] for three European cities with different climatic conditions.

4.2. ECO-Driving

ECO-driving is an energy-saving technique that utilizes velocity modification to achieve smoother changes in velocity using ramped acceleration. This acceleration is made

more manageable by the EVs' tractive powertrain; thus, the vehicle can efficiently and more accurately track the modified velocity profile, unlike ICE-based vehicles. To implement an efficient ECO-driving strategy, the velocity modification takes the following steps to reduce the energy expenditure of the vehicle:

- Avoid sudden acceleration and deceleration using a ramped approach.
- Limit the maximum acceleration to 1 m/s^2 .
- Limit the maximum velocity to 15 m/s .
- Ensure that the distances tracked by both velocity profiles (i.e., the original velocity profile and the eco velocity profile) are synchronized.

Figure 13 illustrates how the velocity modification approach is implemented in the simulation using the abovementioned criteria, resulting in smoother changes in the vehicle speed, while, at the same time, ensuring that the same distance is tracked by the vehicle.

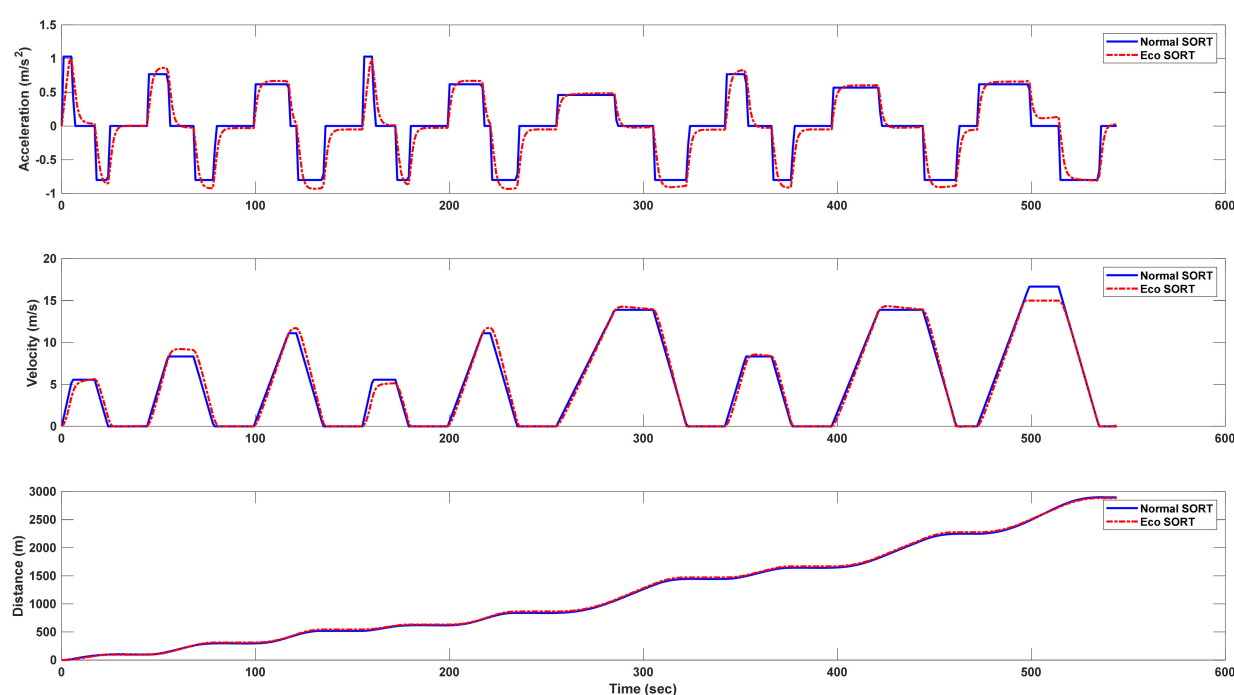


Figure 13. ECO-driving profile generated for a standard driving cycle [26].

The second method by which the ECO-driving technique can improve the energy efficiency of the vehicle is by optimizing the regenerative braking strategy (RBS) by actuating the electric motor in various modes during the braking process. In [26], the different modes of actuation are described in detail, and the resulting ability of the vehicle to track a given velocity profile under the various modes is evaluated and compared. It is shown that, depending on the specific situation, a given mode of actuation will perform better. Thus, the best method to recover the maximum energy from regenerative braking involves continuously tuning the mode of actuation, depending on the (1) current velocity of the vehicle, (2) the desired deceleration, and (3) the grade of the road. Furthermore, RBS is only effective in recovering energy when the vehicle has sufficient momentum; therefore, it is implemented only if the vehicle is decelerating from speeds greater than 5 m/s . For this reason, the energy savings achieved using ECO-driving is highly dependent on the average velocity of the E-bus traveling on a given route. Therefore, buses driving on routes H16 and L33 in Barcelona, where the average route velocities are lower (Table 5), are expected to have less energy savings due to ECO-driving, as compared to the buses driving on routes R55 and EL16 in Gothenburg, where the average route velocities are higher (Table 6), which will have higher energy savings due to ECO-driving.

4.3. ECO-Charging

ECO-charging is an energy-saving technique that can be used during battery charging to reduce the battery cooling energy expenditure using pulsed charging, instead of continuous charging. The frequency and duty cycle of the pulses have been tuned via optimization to achieve a combination that provides the minimum energy expenditure for battery cooling, as shown in Figure 14.

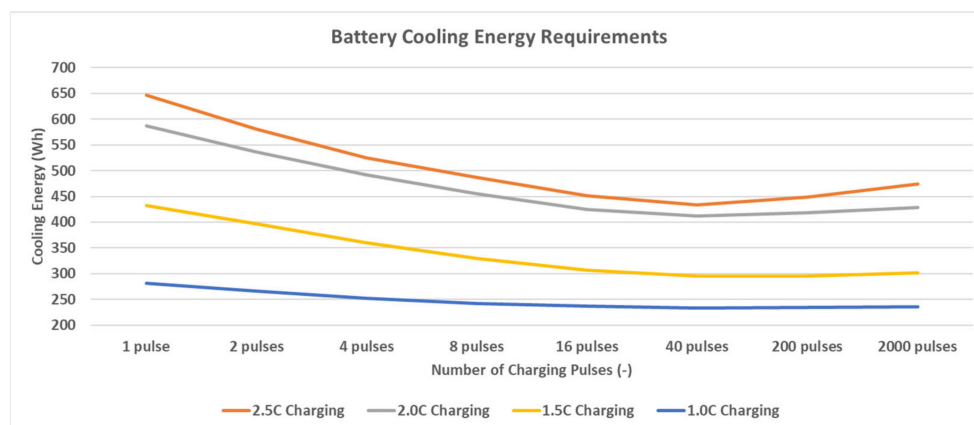


Figure 14. Battery loss as a function of the charging pulses and charging rate.

Figure 14 shows the cooling energy required to keep the battery temperature within its optimum operating temperature range, when it is being charged for a total duration of 600 s and allowed a total duration of 1400 s to cool down. However, the mode of charging can either be continuous, i.e., one pulse, or the charging can be broken up into multiple pulses with an equal duration. Regardless of the size of the pulse used, the total charging duration remains 600 s, and the total cooldown periods remains 1400 s. The figure shows that the minimum cooling energy is required when there are 15-s pulses, followed by a 35-s cooldown period. This reduction in the cooling energy can be explained by the fact that during pulsed charging, the share of the passive cooling is higher, as heat is not continuously generated due to power losses; for continuous charging, there is a continuous generation of heat, leading to a more active cooling by the HVAC system.

Furthermore, as Figure 14 shows, there are significant energy savings when the pulsed charging technique is implemented for high C-rate charging, whereas low C-rate charging does not see much benefit. Thus, it is desirable to implement pulsed charging in opportunity chargers, while overnight chargers can use continuous charging. Low C-rate charging requires less battery cooling than high C-rate charging, because in low C-rate charging, less current is used during charging, resulting in fewer losses due to the series resistance of the ESS. Thus, ECO-charging also attempts to maximize the utilization of the overnight charger for charging by minimizing the time the E-bus spends charging at the opportunity charger. This allows the SoC of the ESS to drift down towards the minimum allowable SoC by the end of the day, and the overnight charger is then used to bring the SoC of the ESS back to its maximum, as shown in Figure 15.

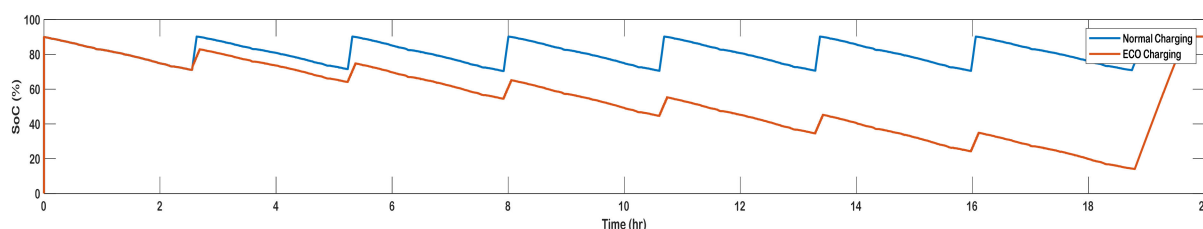


Figure 15. The SoC profile of the ESS charged using the ECO-charging technique.

The paper investigates the seasonal effects of climate on the ECO-charging technique described in [20] and the cooling power needed to keep the ESS within their optimum operating ranges. Colder temperatures will aid in battery cooling; thus, it takes longer for the battery temperature to exceed a predefined setpoint, which will activate the ECO-charging process; thus, the charging tends to be continuous in cold weather. One of the downsides of ECO-charging is that battery charging takes longer to complete, leading to costs associated with not following the bus schedule; however, the reduction in energy expenditure, combined with the increase in battery longevity, compensates for it. ECO-charging has another advantage when implemented on a large scale: groups of opportunity chargers can be synchronized, so that even when they operate simultaneously, the load on the grid is only that of a single opportunity charger. The CMS can do this by phase shifting the charging pulses, so that when one charger is charging a vehicle, the others in the group are idling.

5. Multi-Objective Optimization Strategy

Optimization is an integral part of the design strategy; it offers the best solutions, while also respecting the key constraints in a problem formulation. In [27], optimization was used for the electrification planning of electric bus fleets to determine the type and number of chargers and electric buses in the city of Dubrovnik, Croatia. Similarly, in [28], optimization was used to estimate the total number of electric buses and charging resources in the design of a full bus network in the city of Guadalajara, Mexico. This paper presents the results and analysis of all the UC simulations of E-buses in the ASSURED project for the cities of Barcelona and Gothenburg, including single bus simulations and fleet simulations. However, these simulations were carried out in compliance with the specifications provided by the OEMs of the E-buses and the chargers and to fulfil the requirements of the CBOs. Nevertheless, it is also of interest to determine the best or optimal configuration of H/W, which will minimize two key parameters that are of interest to the CBO and the distribution system operator (DSO), namely, the TCO and the impact on the local grid. One way to do so is by implementing the ECO-strategies described in the previous section. In this section, an optimization approach will be considered to determine which H/W configuration results in the least TCO and grid impact.

The optimization parameters to be considered are the rated power of the opportunity and overnight chargers, the duration of opportunity charging, the number of opportunity chargers, and the duration of the charging pulse (when ECO-charging is considered). Since the optimization process takes a very long time to complete for large fleets of vehicles (36 E-buses in Barcelona and 20 E-buses in Gothenburg), it was performed only for the worst mission scenario, which for Barcelona occurs during the month of July (heavy cabin cooling required), while for Gothenburg, it occurs during the month of January (heavy cabin heating required). Furthermore, the optimization was completed without any ECO features and with all the ECO features activated. The results were compared with the appropriate UC fleet results. Finally, the fleet optimization encompassed all the routes of a given city.

The optimization algorithm, implemented in [20], is used in this study, but with the following key differences:

- Four types of buses, including two 12 m buses and two 18 m buses, are considered in this paper, while the buses in the previous research were all the same type.
- Unique charging durations are considered in this paper for each bus type, while in the previous study, a single charging duration was used for all buses.
- The previous research only considered one bus route in one city, while this paper studies two cities with completely different climates and two routes within a city that have different characteristics to each other in terms of the speed, grade, and bus schedules.

- The previous study considered only discrete power levels for opportunity and depot chargers, which limited the optimized results; therefore, in this paper, the power level of the charger is continuously varied within constraints.
- The previous research only considered optimization without considering the ECO-strategies, while this paper also studies the effect of ECO features on the optimization result.

Other than the differences listed above, this paper also modifies the optimization algorithm to feature a novel convergence criterion to exit the iterative loop. Despite the improvements considered in this paper, there are still some deficiencies, including the fact that all the ESS components are considered to be new and have full capacity, and the effects of battery ageing on the optimization process have not been studied. The effect of battery sizing in terms of the energy needs has also not been considered.

5.1. Improved Simple Optimization Using a Novel Convergence Strategy

Simple optimization (SOPT) is a meta-heuristic algorithm, like the Genetic Algorithm, which uses a random set of parameter values within the solution space to ensure that that optimization result does not get stuck in a local minimum. SOPT consists of an exploratory and an exploitation stage within each iteration, represented by the controlling parameters, c_1 and c_2 . The value of c_2 is set as half of the value of c_1 to lessen the dependency of the algorithm on these controlling variables, and c_1 is set to be between 1 and 2 to decrease the number of iterations required to reach the optimum solution. Equations (8) and (9) describe the method used to calculate a new solution during each iteration, and Figure 16 depicts a flowchart describing the algorithm.

$$x_{i,m,new} = x_{i,m,best} \pm c_1 \times R_{i,m} \quad (8)$$

$$x_{i,m,new} = x_{i,m,best} \pm c_2 \times R_{i,m} \quad (9)$$

where $x_{i,m,best}$ is the value that represents the best solution in the current iteration, i , for a given optimization parameter, m , and $R_{i,m}$ is a randomly generated number that is normally distributed around zero, with a standard deviation of σ_m for that parameter in the solution space. The solution space, n , is an array maintained to hold the best combinations of optimization parameters, i.e., the combinations that give the lowest values for C_{TOT} . To ensure sufficient variability within the optimization parameters, for the size of n , $n \geq (m + 1)$ or $n \geq 10$, whichever is greater. The maximum number of iterations, d , is set to 50, after which the optimization will stop. In each iteration, four new solutions are considered. Since the solutions are independent of each other, they can be simulated in parallel to improve the optimization speed by a factor of four. To improve the SOPT algorithm (iSOPT) and ensure that the best solution is truly a global minimum, the best solution is replaced by a new randomly generated solution if the best solution remains unaltered for a certain number of iterations, R_c , given by Equation (10).

$$R_c = 0.5 \times m \times n \quad (10)$$

where m is the number of optimization parameters, and n is the size of the solution space.

In [29], the SOPT algorithm handles constraints by calculating two fitness scores that must be minimized, the optimization fitness score, based on the minimization of the desired output, and a constraint fitness score, which checks how well the value for each optimization variable falls within their given constraints. The minimization of the constraint fitness score is prioritized above the minimization of the optimization fitness score to ensure that the optimized solution does not contain values that fall outside its parameter's constraints. However, in this paper, for simplicity, instead of calculating a

separate fitness score for the constraints, all the newly calculated values in Equations (8) and (9) are bound within their constraints during each iteration, as shown in Equation (11).

$$x_{i,m,new} = \begin{cases} UB_{i,m} & \text{if } x_{i,m,new} > UB_{i,m} \\ LB_{i,m} & \text{if } x_{i,m,new} < LB_{i,m} \\ x_{i,m,new} & \text{otherwise} \end{cases} \quad (11)$$

where $UB_{i,m}$ and $LB_{i,m}$ are the upper and lower bounds of the constraints, respectively. Once the new optimization parameters are simulated, the result is added to the solution space. Then, the combined set is sorted, and the worst four results are discarded.

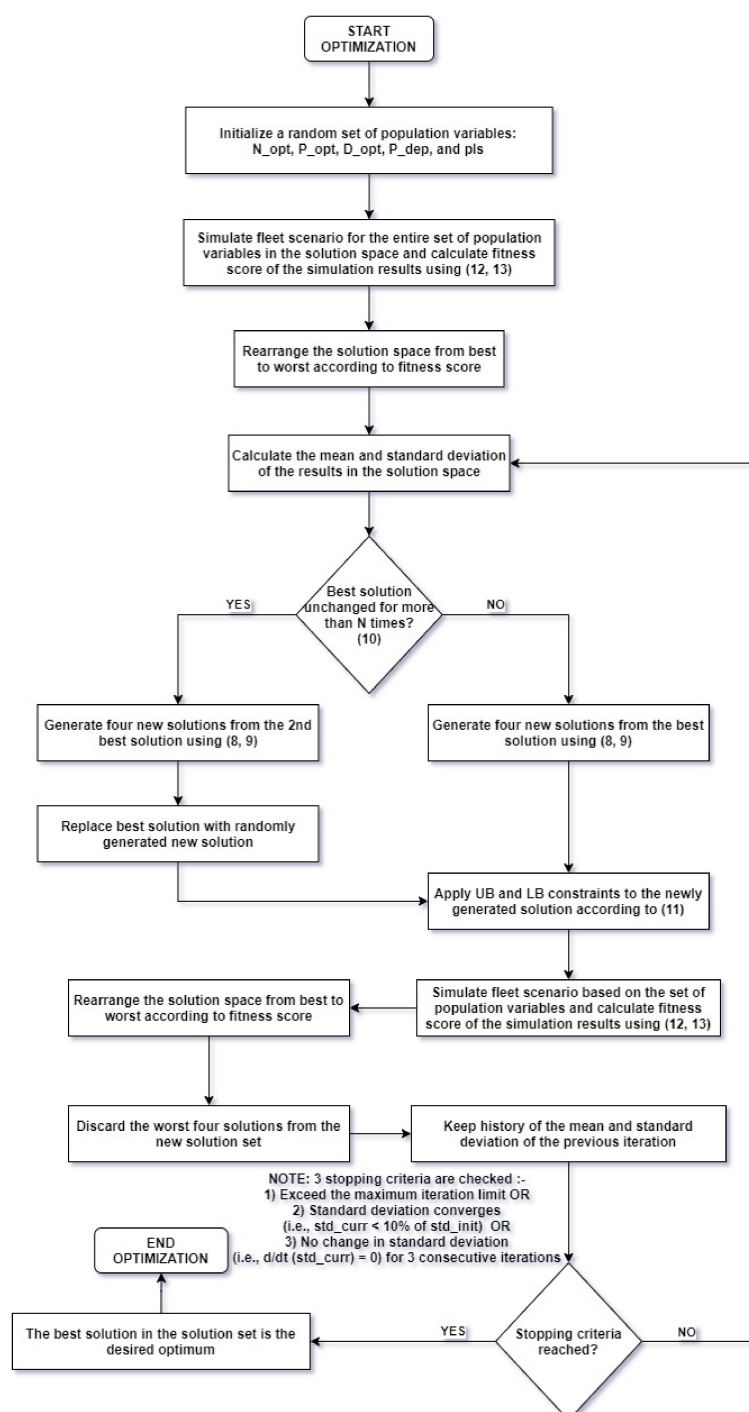


Figure 16. Flowchart describing the iSOPT algorithm.

This paper introduces a novel convergence strategy into the iSOPT algorithm, which will allow it to exit the iterative optimization loop. After every iteration, as the solution space is updated with the best solutions, the standard deviation of the optimization parameters within the solution space keeps decreasing. The algorithm will monitor the sum of the standard deviation, $\Sigma\sigma_m$, of all the optimization parameters, and if they fall below 10% of the initial $\Sigma\sigma_m$, or if the derivative of the $\Sigma\sigma_m$ is zero for three consecutive iterations, then it is assumed that the solution has converged, and the algorithm will exit the iterative optimization loop. Figure 16 illustrates the iterative process of the iSOPT algorithm. The iSOPT algorithm is initialized with a random population set of the optimization variables in the solution space. Five variables are considered in this paper: the number of opportunity chargers, N_{opt} , opportunity charger power level, P_{opt} , opportunity charging duration, D_{opt} , overnight charger power level, P_{dep} , and ECO-charging pulse duration, pls . Each bus type in the fleet is represented with its own D_{opt} , and each route has its own N_{opt} and P_{opt} . Thus, there are multiple values of these optimization parameters.

The number of depot chargers and the charging duration of the depot chargers are dependent on other simulation factors and are thus not considered for optimization. Each optimization parameter is initialized with random values, which are uniformly distributed between their upper and lower bounds. Out of the five optimization variables, only N_{opt} , the number of opportunity chargers, is a discrete variable, while the remaining four variables are continuously varying and can take any values in between their upper and lower bounds. For the discrete optimization parameters, N_{opt} , the value calculated using Equations (8) and (9), i.e., $x_{i,m,new}$, will be rounded to the nearest integer, which will ensure that the number of chargers required is not a fractional value. Table 8 lists the upper and lower bound for each parameter and other constraints.

Table 8. The simulation constraints for the fleet based on the OEM and CBO requirements.

Parameter	Lower Bound	Upper Bound	Parameter	Lower Bound	Upper Bound
Barcelona			Gothenburg		
N_{opt_L33}	1	2	N_{opt_R55}	1	2
N_{opt_H16}	1	2	N_{opt_EL16}	1	2
P_{opt_L33}	200 kW	600 kW	P_{opt_R55}	200 kW	600 kW
P_{opt_H16}	200 kW	600 kW	P_{opt_EL16}	200 kW	600 kW
P_{dep}	50 kW	150 kW	P_{dep}	50 kW	150 kW
pls	5 s	45 s	pls	5 s	45 s
$D_{opt_L33_Type1}$	60 s	420 s	D_{opt_R55}	60 s	600 s
$D_{opt_L33_Type2}$	60 s	420 s	D_{opt_EL16}	60 s	300 s
$D_{opt_L33_Type3}$	60 s	420 s			
$D_{opt_L33_Type4}$	60 s	420 s	SoC constraints		
$D_{opt_H16_Type1}$	60 s	480 s	Barcelona	15%	100%
$D_{opt_H16_Type2}$	60 s	480 s	Gothenburg	10%	90%
$D_{opt_H16_Type3}$	60 s	480 s			
$D_{opt_H16_Type4}$	60 s	480 s			

The iSOPT algorithm used in [16] will be used here to minimize the cost function shown in Equation (12), defining the weight given to each objective towards the overall score.

$$C_{TOT} = \text{Grid_day} \times \Sigma(\text{TCO_fleet}) / \Sigma(\text{NRG_fleet}) \quad (12)$$

$$C_{TOT} = C_{TOT} + \Sigma(e^{\text{SoC_LB}} - \text{SoC_Min}) + \Sigma(e^{\text{SoC_UB}} - \text{SoC_Fin}) \quad (13)$$

where TCO_fleet is the average total cost of operation of the fleet (€/km), NRG_fleet is the average energy utilization of the fleet (kWh/km), and Grid_day is the daily cumulative energy consumption from the grid (kWh). The unit of C_{TOT} is €, which is the modified energy tariff. The second part of the cost function, C_{TOT} , is the penalty function applied when the simulation results exceed the constraints. There is a strict requirement to fulfil the

SoC requirements of the ESS; these constraints are placed by the OEM to ensure a normal operation of the ESS. If the daily minimum SoC falls below the SoC lower bound, then an exponential penalty is applied to the excess. Furthermore, it is a requirement that the ESS is fully charged to its upper bound SoC by the end of the day, and if the simulation fails to do so, another exponential penalty is added to the cost. This ensures that the simulation respects the constraints placed by the OEM and the CBO.

The algorithm allocates the highest priority to TCO minimization, followed by grid impact and vehicle energy utilization, to calculate the overall score, which is minimized. The goal of the algorithm is to determine the optimal number of opportunity chargers, the rated power of the opportunity and overnight charger, as well as the opportunity charging duration that will minimize C_{TOT} .

5.2. Monte Carlo

Monte Carlo simulation is a statistical technique by which a quantity is calculated repeatedly, using randomly selected input configurations for each simulation [30]. Typical Monte Carlo simulations are performed to find the likelihood of all possible outcomes; however, in this paper, the Monte Carlo simulation was performed as a “brute-force” technique to compare the results of iSOPT and validate the results of the optimization. The input parameters randomly vary between the upper and lower bounds of a uniform distribution. The upper and lower bounds are presented in Table 8. To have sufficient confidence in the outcome of Monte Carlo simulation, it is necessary to take a large sample size to ensure that all possible input combinations are covered. However, since each individual simulation takes a set amount of time to complete, the sample size cannot be too high; otherwise, the entire Monte Carlo simulation will take an excessively long time to complete. Nevertheless, Monte Carlo simulations can be accelerated using parallel processing, as individual simulations are independent of each other and do not share data. Using the command, “parsim”, in MATLAB, individual simulations can be launched in parallel, and for a typical octo-core processor, seven simulations can be run in parallel, leaving one core for supervisory purposes. For this paper, a sample size of 250 was used for the Monte Carlo process for the Barcelona fleet simulation and 500 for the Gothenburg fleet simulation; since the fleet size in Barcelona is twice the size of the Gothenburg fleet size and thus takes almost double the time to complete, the number of simulations are halved.

The cost function defined in Equation (12) is used to evaluate the suitability of each input combination, and the results are sorted to determine the best input combination that will result in the lowest cost.

6. Results and Discussion

This section presents the results of the UC simulations for single buses and fleets, as well as the results of the optimization. The effects of the ECO features are also considered.

6.1. Use Case Results for Single Buses

For the single bus results, a series of figures depict the performance of the ESS in meeting the energy demands of the vehicle while complying with the UC. Figures 17–19 present the typical power demands for routes L33 and H16 in Barcelona and route R55 in Gothenburg, respectively, based on the vehicle complying with a given mission profile in Section 3. Since the worst power requirement is being considered, the result for Barcelona is shown for summertime, while the result for Gothenburg is shown for wintertime. Figures 20–22 present the SoC response of the ESS for these power profiles, when the charging duration at the opportunity charger is minimized.

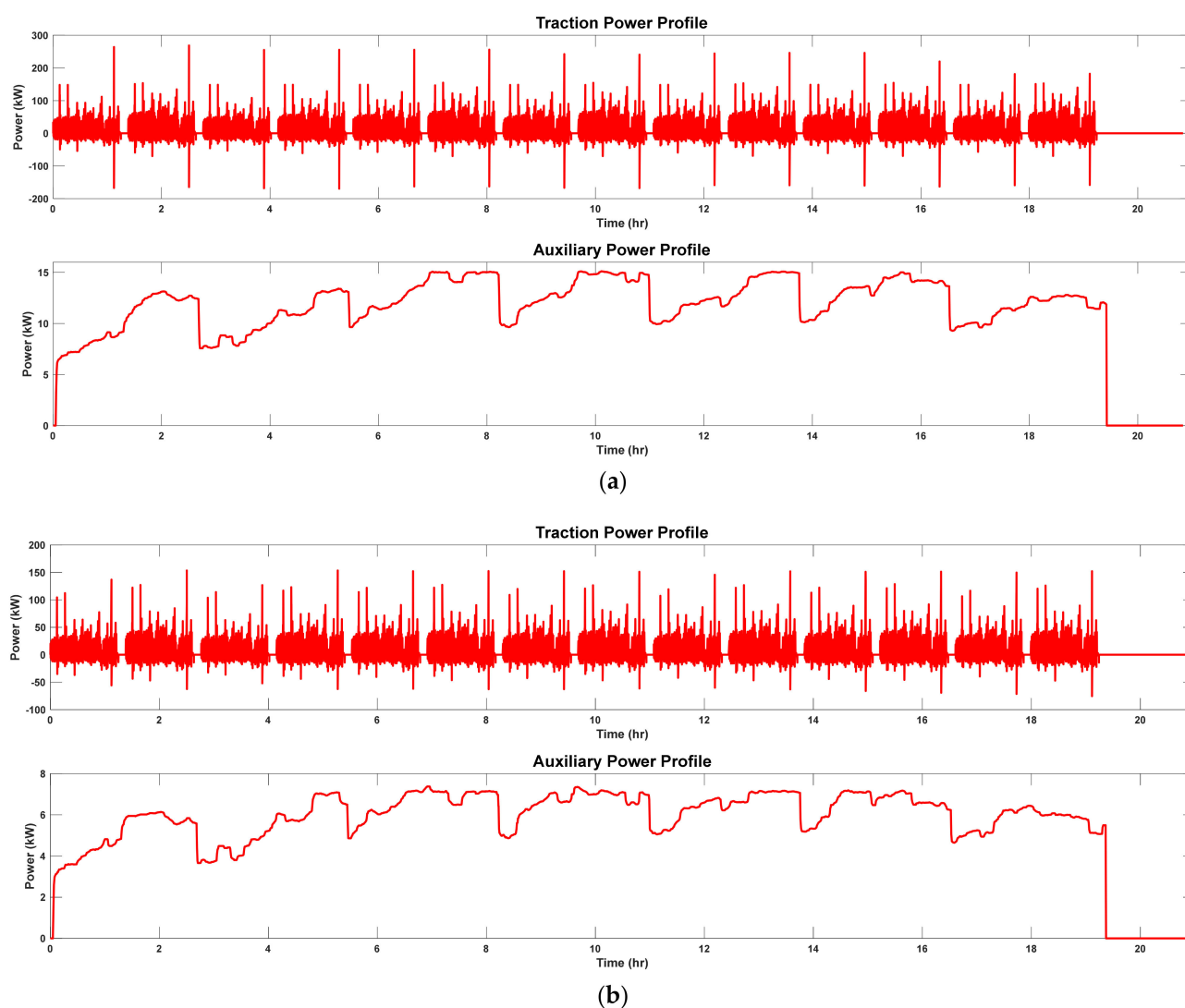


Figure 17. Power requirement for route H16, Barcelona for (a) an 18 m bus (Type 1, 3) and (b) a 12 m bus (Type 2, 4).

The simulation assumes that the entire duration allowed for charging (see Tables 5 and 6) and that the E-bus is charged once per return trip. It can be observed that the capacity of the ESS in the 18 m buses is barely sufficient to cover the energy requirements for one return trip, more than 40% DoD in Barcelona route L33, and more than 60% DoD in Barcelona route H16; however, it is compensated by the fact that the battery chemistry of the bus's ESS allows for really fast charging (see Table 7) and the battery can thus get fully charged within the allocated charging duration, when a superfast opportunity charger (600 kW) is used. On the other hand, the 12 m buses have ESS capacities that would allow for 3 return trips without charging in Barcelona route H16 and 4 return trips without charging in Barcelona route L33 and Gothenburg route R55, so there can be flexibility in their charging schedule. The CMS can either allocate a lower priority for charging for the 12 m buses if the grid is overloaded when the bus requires charging, so the bus can either skip charging or the bus can be charged for shorter durations, i.e., a quick top-up charge. Table 9 lists the seasonal energy requirements for the buses in cities driving in normal mode, while Table 10 lists the TCO values. The effects of the ECO features are discussed in the following subsection.

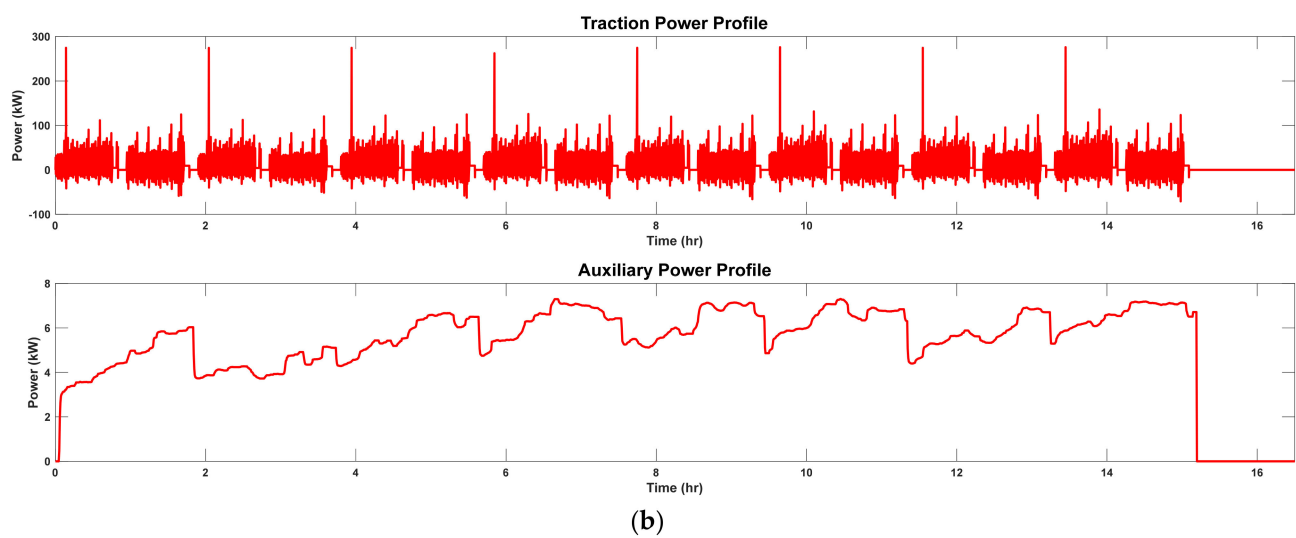
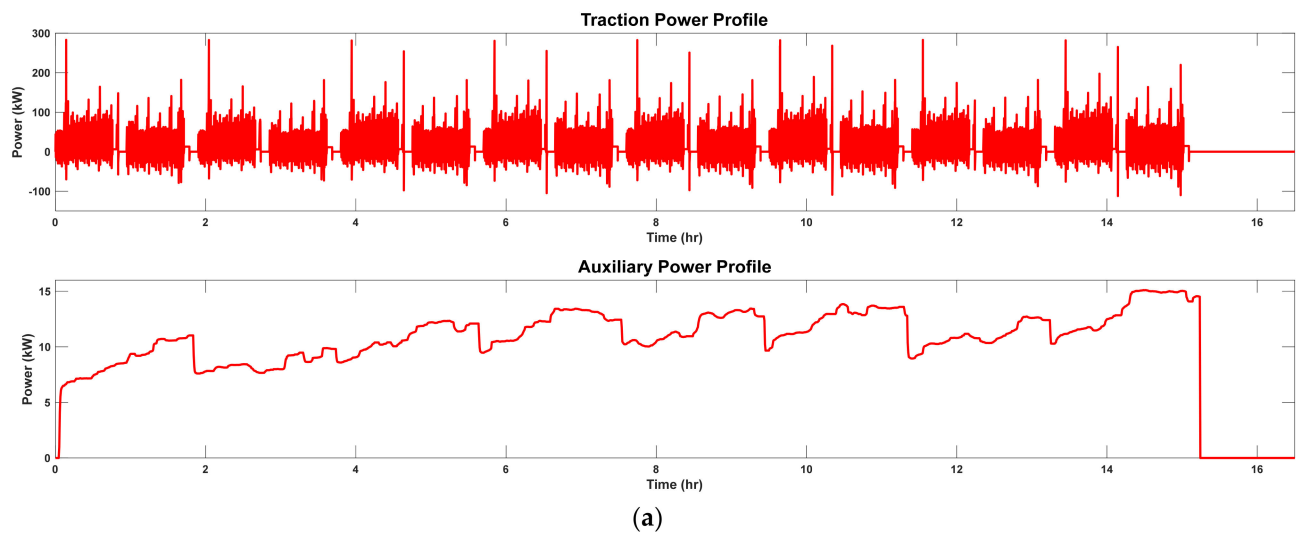


Figure 18. Power requirement for route L33, Barcelona for (a) an 18 m bus (Type 1, 3) and (b) a 12 m bus (Type 2, 4).

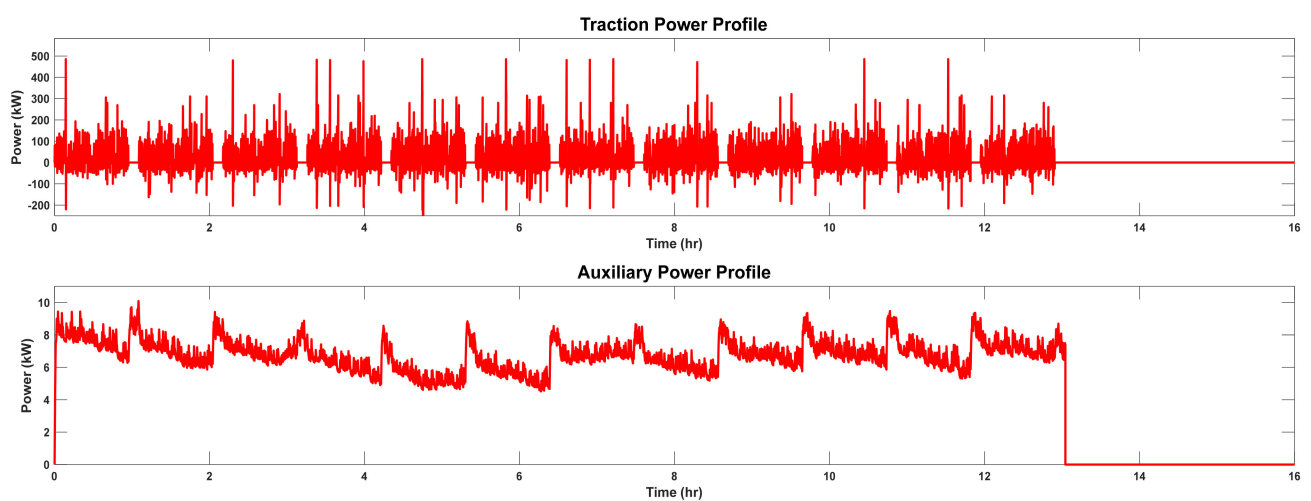


Figure 19. Power requirement for route R55, Gothenburg for a 12 m bus (Type 2).

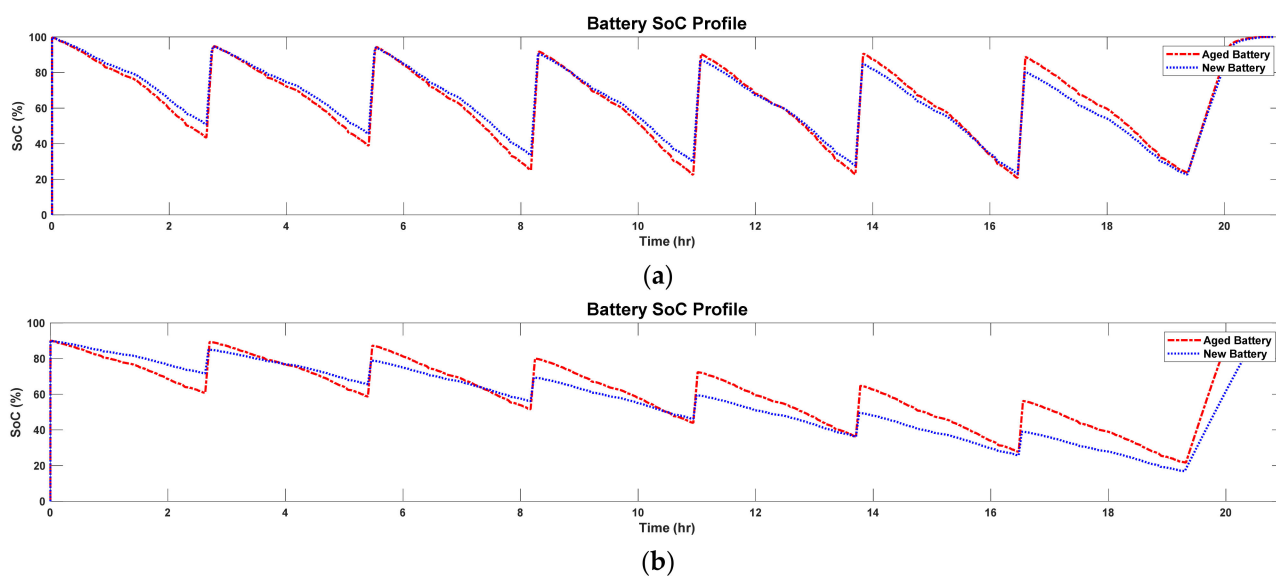


Figure 20. The ESS SoC profile of route H16, Barcelona for (a) an 18 m bus (Type 1, 3) and (b) a 12 m bus (Type 2, 4).

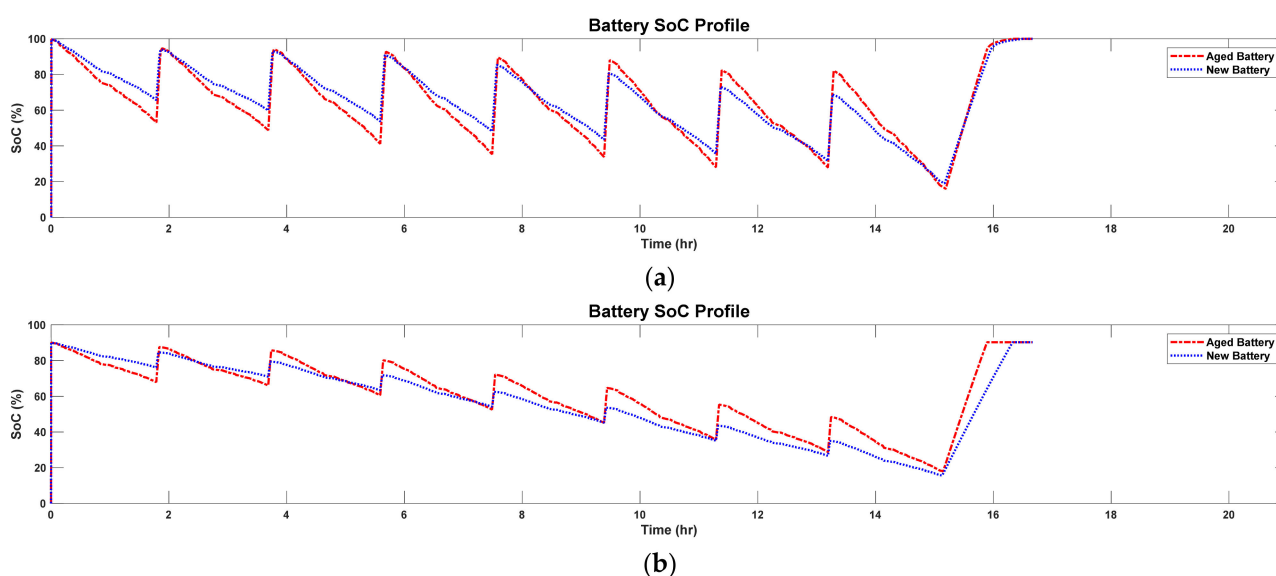


Figure 21. The ESS SoC profile of route L33, Barcelona for (a) an 18 m bus (Type 1, 3) and (b) a 12 m bus (Type 2, 4).

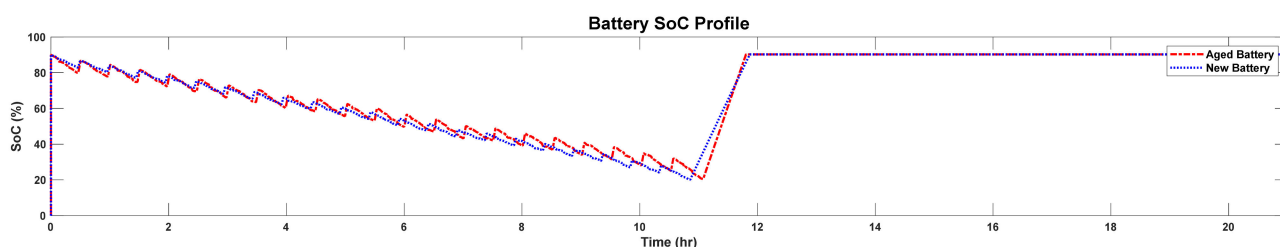


Figure 22. The ESS SoC profile of route R55, Gothenburg for a 12 m bus (Type 2).

An interesting fact that can be observed is that for hotter climates the energy requirement is greater during the summer and lower during the winter; however, for colder climates, it is the reverse. The route's elevation and speed profile also have an impact on the energy requirement, with L33 generally requiring less energy than H16, while R55 has the lowest energy requirement. Finally, the results show that 18 m buses have greater than 50% higher energy requirements, compared with 12 m buses.

Table 9. Seasonal energy usage rate (in kWh/km) of buses for different cities and routes.

Bus	Barcelona		Gothenburg
	Route L33	Route H16	Route R55
Summer			
Type 1	2.26	2.56	–
Type 2	1.50	1.54	1.46
Type 3	2.32	2.62	–
Type 4	1.37	1.47	–
Winter			
Type 1	1.83	1.94	–
Type 2	1.37	1.39	1.92
Type 3	1.98	2.13	–
Type 4	1.16	1.20	–

Table 10. Seasonal TCO (in €/km) of buses for different cities and routes.

Bus	Barcelona		Gothenburg
	Route L33	Route H16	Route R55
Summer			
Type 1	1.77	1.78	–
Type 2	1.32	1.21	1.29
Type 3	1.53	1.41	–
Type 4	1.41	1.41	–
Winter			
Type 1	1.76	1.77	–
Type 2	1.32	1.21	1.30
Type 3	1.52	1.40	–
Type 4	1.40	1.40	–

6.2. Use Case Results for Bus Fleets

While the single bus results are presented from the vehicle point of view (POV), the results for the fleets are presented in terms of their impact on the local grid. Figure 23 presents the load profile on the local grid for the city of Barcelona during summer and the load profile on the local grid for the city of Gothenburg during winter. Two different seasons were chosen for the cities not to compare the seasonal effects, but because the aim is to present the worst load that the grid will experience for each city. For a hot climate like Barcelona, the worst load occurs during summertime, while for a cold climate like Gothenburg, the worst load occurs during wintertime. With prior knowledge of the bus schedules, the grid load profile for Barcelona and Gothenburg gives an indication of how many chargers are actively charging at any given moment.

As mentioned in Tables 5 and 6, the city of Barcelona was simulated with two opportunity chargers (FC in Figure 23) and four overnight chargers (OC in Figure 23), while the city of Gothenburg was simulated with four opportunity chargers and three overnight chargers. Furthermore, Figure 23 shows the effect of charging different types of buses (Barcelona), compared with charging a single type of bus (Gothenburg). The load profile of Gothenburg appears more consistent in the load pattern than that of Barcelona. Additionally, in Barcelona, the ESS of 18 m E-buses are charged to 100% SoC. Thus, they experience constant voltage charging for part of the time, which appears as exponential decay curves in the profile. On the other hand, in Gothenburg, all ESS are charged to only 90%. Thus, the charging pattern is that of constant current charging.

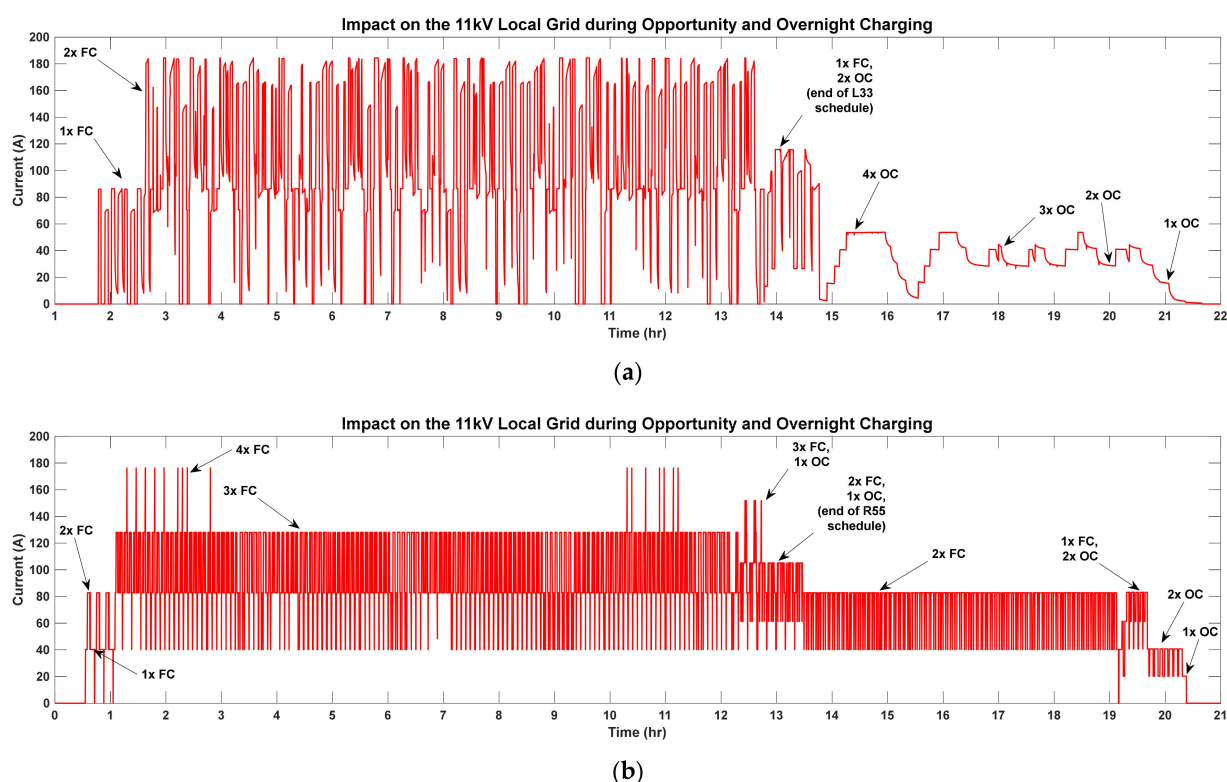


Figure 23. Grid electricity consumption profile by the fleets of E-buses in the cities for (a) Route L33 and H16 in Barcelona during summertime and (b) Route R55 and EL16 in Gothenburg during wintertime.

Table 11 shows the energy requirements and the TCO for the two cities. One final observation in the figure that is worth noting is the current load on the grid. In Barcelona, 600 kW superfast chargers are used during opportunity charging. Thus, when two chargers are active simultaneously, the grid experiences a load of 180 A of current. Conversely, in Gothenburg, 290 kW fast chargers are used as the opportunity charger. Thus, it requires all four chargers to be active simultaneously to exert the same load on the grid, which happens infrequently. In this regard, from the grid POV, it makes more sense to have two 290 kW opportunity chargers with twice the charging duration allocated, instead of one 600 kW opportunity charger.

Table 11. Comparison of the energy requirement and TCO for the fleets of buses.

	Barcelona		Gothenburg	
	Winter	Summer	Winter	Summer
Grid Impact (MWh)	10.7	13.5	15.2	12.3
Energy Usage Rate (kWh/km/bus)	1.65	2.07	1.88	1.47
TCO (€/km/bus)	0.93	0.94	0.90	0.89

One interesting fact is that the TCO values shown in Table 11 are much lower than the TCO values provided in Table 10. This is because the TCO in Table 10 is calculated only for one bus, using one opportunity and one overnight charger, while the TCO in Table 11 is calculated based on fleets of buses sharing the same opportunity and overnight chargers. Thus, the capital costs are also shared between the buses, and the average TCO per bus is much lower. As for the energy usage rate, the values provided in Table 11 are the average of all buses and routes for that city in each season.

6.3. Effects of the ECO Features

This subsection presents how ECO features reduce the TCO, grid impact, and energy consumption rate and considers the impact that the driving speed, climate, and charging rate have on the effectiveness of the ECO features. Figure 24 analyzes the effects of ECO-comfort and ECO-driving; from the data, it can be observed that ECO-comfort is more effective as an energy saving mechanism for hot weather. Thus, a warm climate like Barcelona has more energy savings, because the ECO-comfort is higher than in a cool climate like Gothenburg. Furthermore, summertime energy savings are greater than wintertime energy savings. This suggest that the cooling mode is more optimized in the HVAC system than in the heating mode. As for ECO-driving, the energy savings are greater when ECO-driving is activated in a route with higher average speeds. In Barcelona, on route H16, with an average speed of 9.52 km/h, almost no effect is observed, while on route L33, with 11.64 km/h, a modest 5~7% energy saving is achieved. On the other hand, in Gothenburg, the routes have higher average velocities, with route R55, with an average speed of 18.24 km/h, showing 11~12% savings.

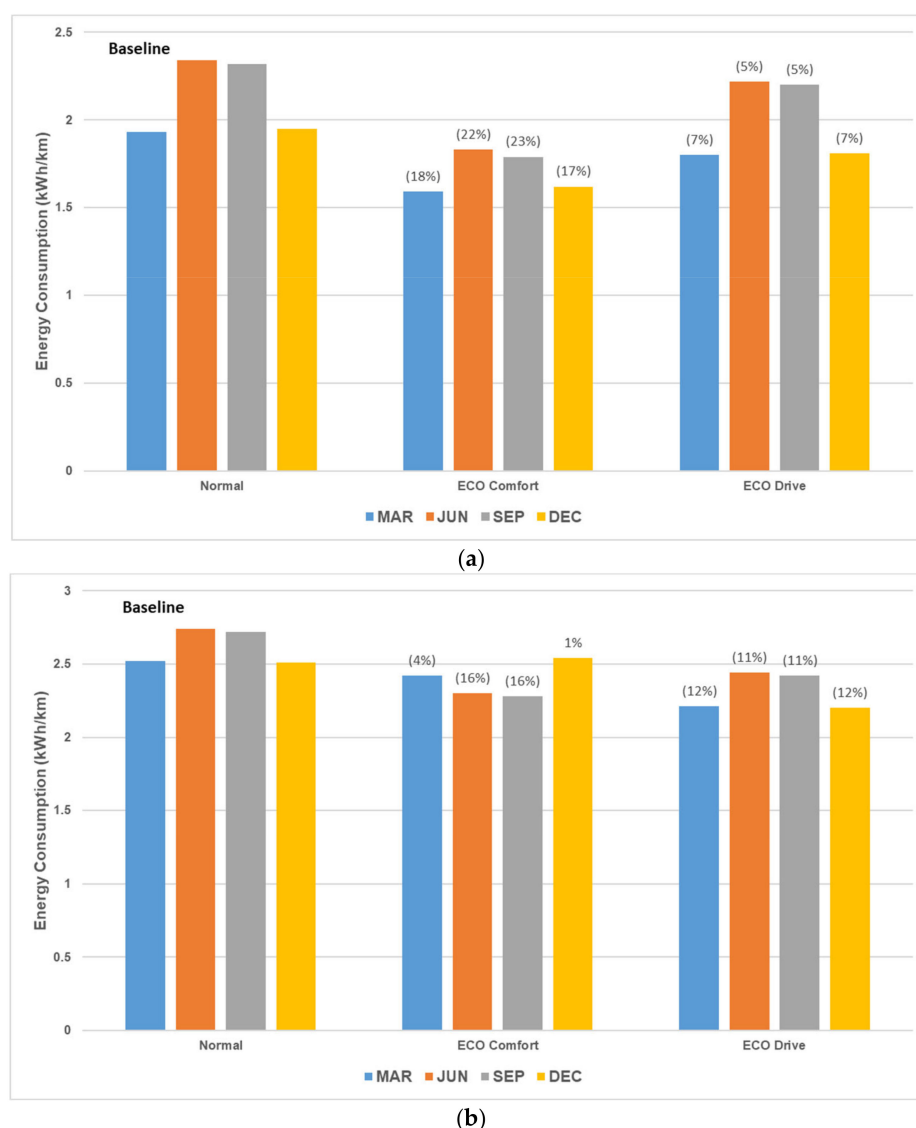


Figure 24. Effect of climate on ECO-comfort effectiveness and driving speed on ECO-driving effectiveness for (a) a Mediterranean climate with average route speed of 3.23 m/s and (b) a Cool temperate climate with average route speed of 5 m/s. In the figure, numbers within brackets represents negative numbers.

Figure 25 visualizes how ECO-charging works on the ESS; it is activated when the temperature of the ESS exceeds a set threshold, which is slightly lower than the threshold when the cooling system will be activated to keep the temperature of the ESS within its normal operational limits. Since ECO-charging is implemented using pulsed charging, the battery gets a chance to cool down naturally in between pulses. This reduces the load on the cooling system. As can be seen from the figure, the required cooling power is lower using ECO-charging and almost non-existent during winter, because the cold weather greatly aids in cooling when the ESS is not actively generating heat. This results in a lower internal temperature, even during high C-rate charging of the ESS. As a result, the electricity consumption for cooling purposes is reduced by up to 17.84%, as can be observed in Figure 26. Furthermore, the reduction is higher for high C-rate charging, charging during winter months, and even in cooler climates. This is because the cold weather will help the battery cool down more effectively than warm weather. It is interesting to note that the climate requirements for the effectiveness of ECO-charging is the opposite of the requirements for the effectiveness of ECO-comfort, even though the same HVAC system is used for both purposes; this is because ECO-charging relies on ambient conditions for cooling purposes, while ECO-comfort must act against those conditions to regulate the temperature in the enclosed cabin.

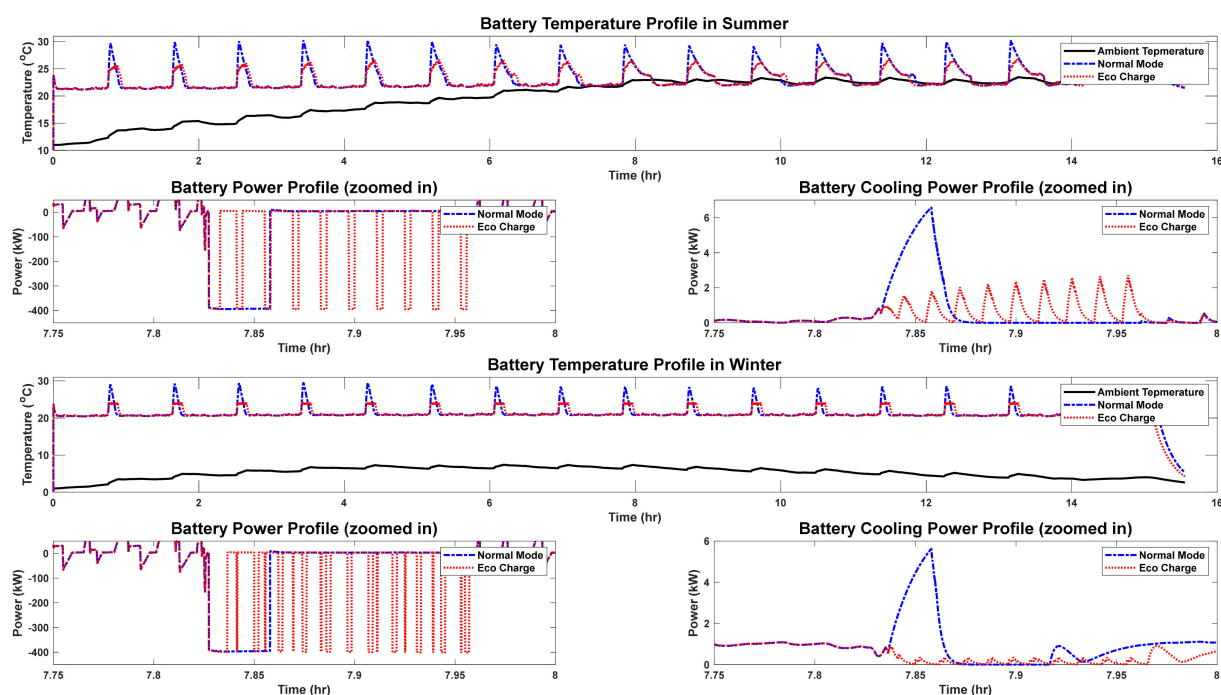


Figure 25. The effect of ECO-charging on the ESS cooling energy requirement.

ECO-charging has one important advantage over the grid POV: it is instrumental in reducing the peak load on the grid. Because ECO-charging is implemented as pulsed charging, it is possible for groups of opportunity chargers to synchronize with each other, so that when one charger is supplying a charging pulse to the ESS, the others will remain idle, i.e., they will timeshare the charging process. Thus, multiple opportunity chargers can be charging simultaneously, while providing a combined load of only one opportunity charger to the grid. Charger synchronization was not developed for this project; however, coincidental timesharing does occur when multiple chargers are in operation using ECO-charging, and this has the effect of lowering the average load on the grid by approximately 10 A to 20 A, compared to normal-mode charging, as shown in Figure 27. Since the reduction takes place during the opportunity charging phase, it must be made up during overnight charging; thus, lowering of the peak grid load leads to spreading out of the

charging duration by transferring it from higher power opportunity chargers to lower power overnight chargers. It should be noted that since an active synchronization of the opportunity charger was not conducted, the load reduction is slight and occurs mainly due to the pulses; with active synchronization, we can expect a significant reduction in the peak grid load. Future research will investigate the extent of this reduction using different charger synchronization techniques.

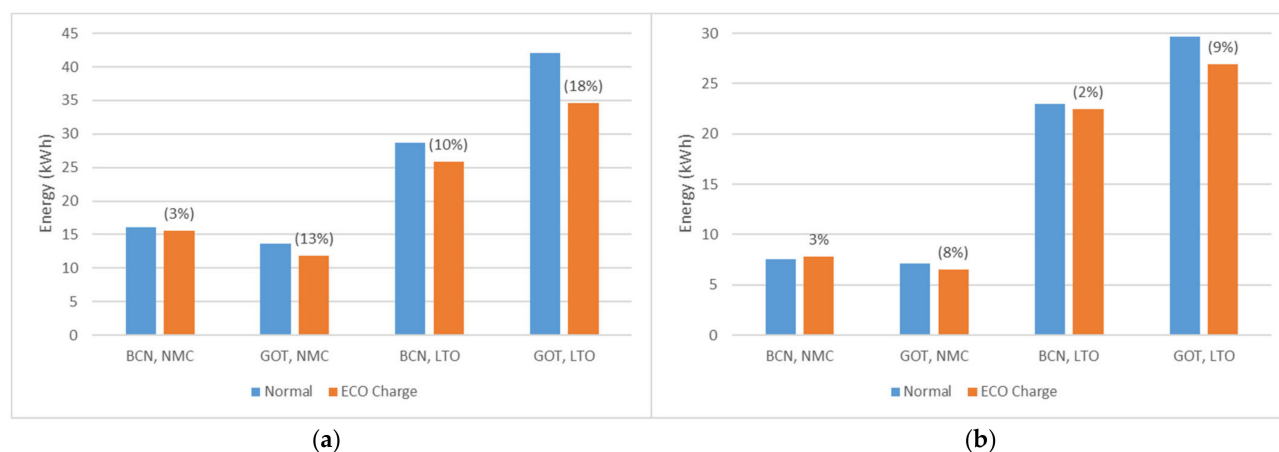


Figure 26. Effect of climate on the ECO-charging effectiveness in reducing the battery cooling energy requirement during (a) Wintertime and (b) Summertime. In the figure, numbers within brackets represents negative numbers.



Figure 27. Effect of ECO-charging on the peak load on the grid.

6.4. Optimization Results

While the previous subsection presented the results for buses and chargers whose configurations were specified by their respective OEMs, this subsection will explore the optimal configurations that would lower the TCO and energy requirements of the entire fleet in a city. The following variables in the fleet configurations were studied: charger power rating, charging duration, number of chargers, and charging pulse duration for ECO-charging, as listed in Table 8. The E-bus parameters were considered to be constant

and unchanging for the purposes of the simulations, although the results could have been made more meaningful if the battery sizing was also considered. Another fact is that the optimization was conducted during the period when the energy requirement was at its worst, which is summertime for Barcelona and wintertime for Gothenburg. Table 12 lists the optimized configuration, simulated as Monte Carlo or iSOPT for Barcelona and Gothenburg.

Table 12. The optimized charger configuration to cover the worst mission scenario.

City of Barcelona		Normal Mode		All ECO Mode	
Monte Carlo		L33	H16	L33	H16
Opportunity chargers (-)		2	2	2	2
Charging duration (s):					
	-Type 2 Bus	112	353	80	80
	-Type 4 Bus	391	261	97	258
	-Type 3 Bus	385	477	354	265
	-Type 1 Bus	380	360	368	347
Opportunity charger power (kW)		296	409	279	277
Overnight charger power (kW)		90		125	
Improved Simple Optimization					
Opportunity chargers (-)		2	2	2	2
Charging duration (s):					
	-Type 2 Bus	91	132	60	217
	-Type 4 Bus	420	331	370	461
	-Type 3 Bus	353	449	215	311
	-Type 1 Bus	270	480	176	480
Opportunity charger power (kW)		267	235	247	200
Overnight charger power (kW)		101		109	
City of Gothenburg		Normal Mode		All ECO Mode	
Monte Carlo		R55	EL16	R55	EL16
Opportunity chargers (-)		2	2	1	2
Charging duration (s):-Type 2 Bus		265	289	356	270
Opportunity charger power (kW)		279	277	203	237
Overnight charger power (kW)		125		79	
Improved Simple Optimization					
Opportunity chargers (-)		1	2	1	2
Charging duration (s):-Type 2 Bus		314	292	181	300
Opportunity charger power (kW)		200	258	209	204
Overnight charger power (kW)		137		86	

The specifications of the OEMs and the CBOs in defining the charging requirements, provided in Tables 5 and 6 are summarized as follows: routes L33 and H16 in Barcelona are serviced by 1×600 kW opportunity charger and 2×100 kW overnight chargers; the maximum opportunity charging duration for route L33 is 420 s, while that of route H16 is 480 s; route R55 in Gothenburg is serviced by 1×150 kW overnight charger and 2×290 kW opportunity chargers, with a maximum opportunity charging duration of 480 s, while route EL16 in Gothenburg is serviced by $2 \times$ overnight chargers and 2×450 kW opportunity chargers, with a maximum opportunity charging duration of 300 s; finally, although 450 kW opportunity chargers are used in route EL16, only a 290 kW charger is utilized to charge the battery, so the charger operates in reduced load conditions. These requirements are highly conservative, and the bus fleets in both cities can do with much less in terms of charging power and charging duration. In Gothenburg, the optimization was successful in identifying a configuration with lower H/W and power requirements, leading to significant cost savings, with the same energy requirements. In contrast, in Barcelona, the optimization algorithms preferred low-power chargers, rather than high-

power chargers, even if the number of required chargers increased as a result. However, the total required charging power still decreased by 16%, compared to the non-optimized version. In opting for lower power chargers, the peak load on the grid also decreases, as discussed in Section 6.2. Figure 28 summarizes and compares the TCO, the vehicle energy usage rate and the total electricity consumption from the grid for the different types of optimization. The TCO and the vehicle energy usage rate is given as the average for the entire fleet for both routes in each city, while the grid impact is the total daily electricity consumption for the city.

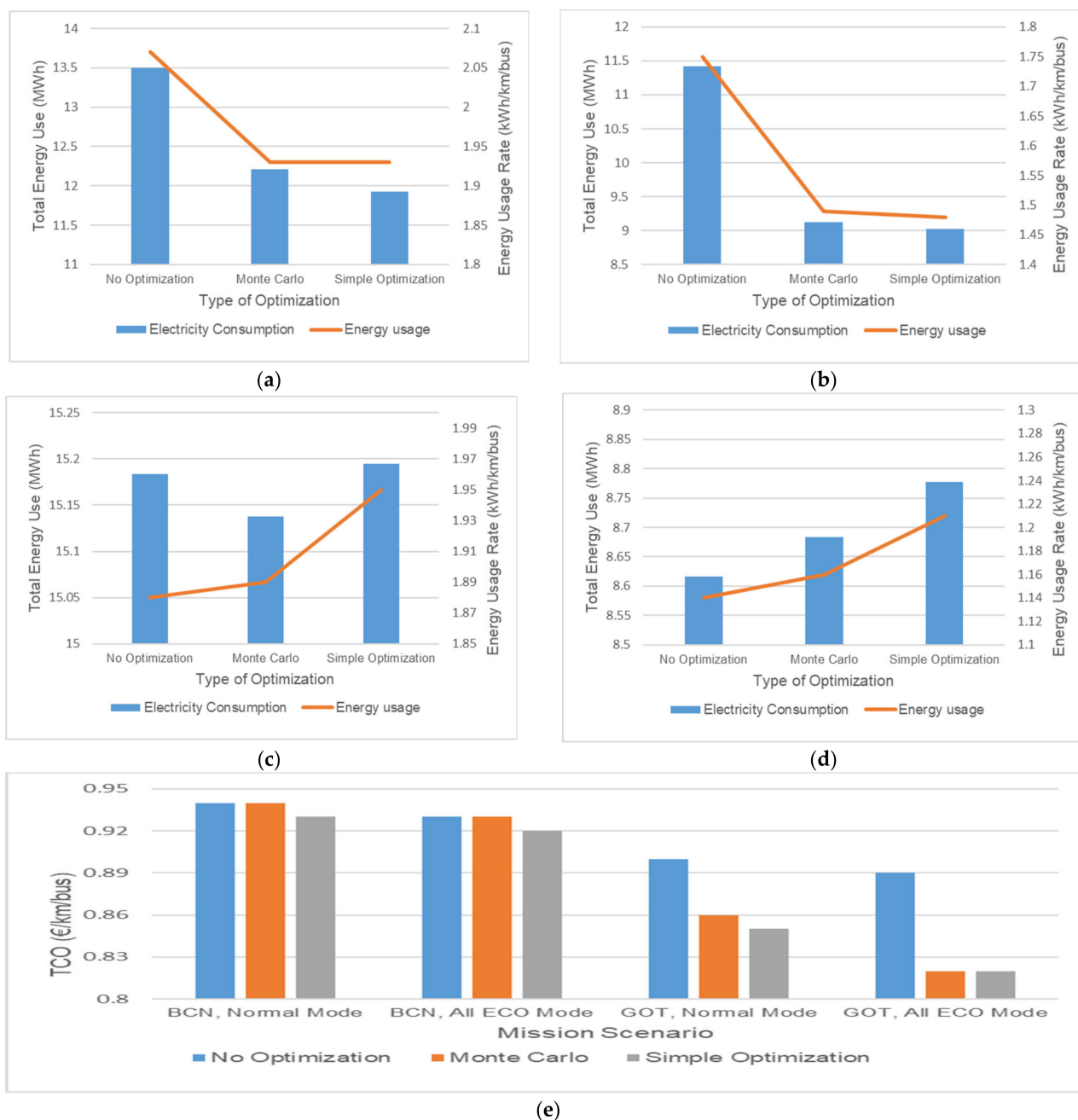


Figure 28. Fleet optimization results for (a) Barcelona in normal mode, (b) Barcelona with all the ECO features, (c) Gothenburg in normal mode, (d) Gothenburg with all the ECO features, and (e) the TCO for all the cases.

It can be concluded, from the data provided in Table 12 and Figure 28, that the charger configuration specified for the city of Barcelona by the OEMs and CBO is not optimal;

in fact, there is significant scope for improvement in terms of energy expenditure, even though the TCO is not so impacted. Thus, many low-powered chargers are better from the grid POV than a small number of very high-powered chargers. On the other hand, the charger configuration specified for Gothenburg by the OEMs and CBO are already in their optimal configuration; however, there is significant scope for reducing the TCO. This is because the 450 kW chargers used on route EL16 have a higher power rating than necessary to charge the vehicle in that route; thus, they can be replaced by 290 kW chargers, leading to significant cost savings.

7. Conclusions

In this paper, a simulation platform was developed using the forward model of an E-bus powertrain to simulate the various UCs of buses in cities participating in the ASSURED project. Simulations for single buses and fleets of buses were presented for the cities of Barcelona and Gothenburg. These two cities were selected for their widely different climates to test the effect of climate on the thermal management using ECO-comfort and ECO-charging. Two routes were simulated in each city, which have widely different speed and elevation profiles, to test their effect on the energy management using ECO-driving. These three ECO features were implemented to evaluate the energy savings that can be achieved compared to the baseline condition. Finally, an optimization was carried out to determine the best combination of charging power, duration, and number of chargers to minimize TCO and grid impact.

The results showed that ECO-driving is more effective when the average velocity of the route is higher, with up to 12% energy savings possible on routes with high average velocities. On the other hand, ECO-comfort optimizes the cooling mode of the HVAC system better than its heating mode. Thus, hotter climates and/or summertime weather see better auxiliary energy savings of up to 23%. Furthermore, ECO-charging is more effective when applied to a higher charging rate (C-rate). Thus, applying ECO-charging to the charging of LTO batteries at 5 C provides a 5% higher energy saving than applying it to the charging of NMC batteries at 2.5 C, and it can reduce the cooling energy requirements by up to 17%. Finally, ECO-charging may also reduce the average load on the grid by more than 10%, even when deploying multiple superfast chargers, and this reduces the need for expensive grid reinforcement strategies.

The results of the optimization strategy indicated that the charging H/W configuration adopted by the CBOs in Barcelona city is over-specified in terms of power levels; thus, a significant saving in the energy requirements was achieved by adopting a more optimal configuration. The optimized H/W configuration can save energy requirements by 11% for the normal mode of operation and 21% when all the ECO-features are applied. Combining the ECO-features, along with the optimized H/W configuration, reduces the energy requirements by up to a third of the baseline energy requirements in Barcelona city. On the other hand, the charging H/W configuration adopted by the CBOs in Gothenburg city is highly expensive; thus, significant savings in the average fleet TCO was achieved by adopting a more optimal configuration. The optimized H/W configuration reduced the average fleet TCO by up to 9% when combined with ECO-features. Finally, the optimization results indicate that using a higher number of low-power opportunity chargers has a lower impact on the grid, on average, than using a smaller number of high-power opportunity chargers.

Future research will study the techniques for opportunity charger synchronization while using ECO-charging to maximize the reduction of the peak load on the grid when multiple superfast chargers are actively charging, without further affecting bus schedules. Future research may also include a sensitivity analysis of deviations in bus schedules, as there generally should be some slag in the overall system to allow for broken chargers, route deviations due to road (re)constructions, and traffic jams. The optimization can be improved by also optimizing the battery size, alongside the charging H/W configuration and ECO-features, to see if further reductions in the total fleet energy utilization and

average fleet TCO can be achieved for a given mission scenario. Finally, future research will consider the lifetime of components based on actual usage, instead of employing the assumptions made in this study, to obtain a more accurate calculation of the TCO.

Author Contributions: M.M.H. was the main author of this manuscript and contributed to the introduction and conclusion, the simulation framework, and the optimization strategy; he was also responsible for the simulations of the bus fleets in Barcelona and Gothenburg and fleet optimization using iSOPT; N.A. contributed to the ECO-comfort methodology; he was also responsible for the single bus use case simulations for Gothenburg city using 12 m buses and the fleet optimization using Monte Carlo; M.R. contributed to the TCO methodology and ECO-charging methodology; she was also responsible for the single bus use case simulations for Barcelona city using 12 m buses; A.S.-d.-I. contributed to the section on the ECO-driving methodology; he was also responsible for the single bus use case simulations for Barcelona city using 18 m buses; M.E.B. contributed to the section on city routes and vehicle types; he was also responsible for ensuring the consistency of the results across different simulation strategies: single bus, bus fleets, ECO features, and optimization; finally, O.H. was the task leader and supervised the research activities; he also liaised with the OEMs and CBOs and was responsible for reviewing the article. Formal analysis: M.E.B.; Investigation, M.M.H., N.A., M.R. and A.S.-d.-I.; Methodology, M.M.H.; Project administration, O.H.; Supervision, O.H.; Writing—original draft, Mohammed Hasan, N.A., M.R., A.S.-d.-I. and M.E.B.; writing—review and editing, M.E.B. and O.H. All authors have read and agreed to the published version of the manuscript.

Funding: This research was funded by the European Commission—Innovation and Networks Executive Agency, grant number 769850, under the title of ASSURED—H2020-GV-2016-2017/H2020-GV-2017.

Institutional Review Board Statement: Not applicable.

Informed Consent Statement: Not applicable.

Data Availability Statement: The complete set of simulation data can be found in ASSURED project WP6 D6.3; however, that source is confidential.

Acknowledgments: The authors acknowledge Flanders Make for their support to this research group. The authors acknowledge the OEMs and CBOs for providing information about buses, chargers, and scenarios.

Conflicts of Interest: The authors declare no conflict of interest.

Abbreviations

BEV	Battery electric vehicle
CBO	City bus operator
CC/CV	Constant current/constant voltage
CCS2	Combined charging system v2
CMS	Charging management system
CO ₂	Carbon dioxide
c-rate	Charging rate
CS	Charging strategy
DoD	Depth of discharge
e-bus	Electric bus
ECO	Economy
EMS	Energy management system
ESS	Energy storage system
EV	Electric vehicle
GHG	Greenhouse gases
HD	Heavy duty
Hi-Fi	High fidelity
HV	High voltage
HVAC	Heating, ventilation, and air conditioning

H/W	Hardware
ICE	Internal combustion engine
iSOPT	Improved simple optimization
LFP	Lithium ferro-phosphate
Lo-Fi	Low fidelity
LTO	Lithium titanate
LuT	Lookup table
MD	Medium duty
MV	Medium voltage
NMC	Nickel-manganese-cobalt
OCV	Open circuit voltage
OEM	Original equipment manufacturer
PF	Power factor
PMV	Predicted mean vote
POV	Point of view
PPD	Predicted percentage dissatisfied
RBS	Regenerative braking system
RCD	Relative capacity degradation
Rp	Polarization resistance
Rs	Series resistance
SoC	State of charge
Tc	Time constant
TCO	Total cost of ownership
TMS	Thermal management system
UC	Use case

Appendix A

The output of the gearbox is given as:

$$T_{GB} = F_T \times R \quad (A1)$$

$$\omega_{GB} = v/R \quad (A2)$$

Traction mode:

$$T_{EM} = T_{GB}/(\eta_{GB} \times K_{GB}) \quad (A3)$$

Regenerative mode:

$$T_{EM} = T_{GB} \times \eta_{GB}/K_{GB} \quad (A4)$$

$$\omega_{EM} = \omega_{GB} \times K_{GB} \quad (A5)$$

where T is the torque (Nm), F is the force (N), ω is the angular speed (rad/s), v is the vehicle velocity (m/s), R is the wheel radius (m), K is the gearbox ratio, and η is the efficiency.

The output of the electric motor and inverter is given as:

$$T_{EM_MAX} = LuT(\omega_{EM}) \quad (A6)$$

$$T_{EM} = \begin{cases} T_{EM_REQ}, & \text{if } -T_{EM_MAX} \leq T_{EM_REQ} \leq T_{EM_MAX} \\ T_{EM_MAX}, & \text{if } T_{EM_REQ} \geq T_{EM_MAX} \\ -T_{EM_MAX}, & \text{if } T_{EM_REQ} \leq -T_{EM_MAX} \end{cases} \quad (A7)$$

$$\eta_{EM} = LuT(T_{EM}, \omega_{EM}) \quad (A8)$$

$$P_{EM} = T_{EM} \times \omega_{EM} \quad (A9)$$

Traction mode:

$$P_{DC_EM} = P_{EM}/\eta_{EM} \quad (A10)$$

Regenerative mode:

$$P_{DC_EM} = P_{EM} \times \eta_{EM} \quad (A11)$$

$$I_{DC_EM} = P_{DC_EM} / V_{DC_EM} \quad (A12)$$

where P is the power (W), T is the torque (Nm), ω is the angular velocity (rad/s), I is the current (A), V is the voltage (V), and η is the efficiency. The T_{EM_REQ} in (A6) is a command sent by the EMS to control the electric motor so that the E-Bus can properly track the velocity profile given in the driving scenario.

The output from the high-power DC-DC converter is given as:

$$\eta_{DC_EM} = LuT(V_{DC_EM}, I_{DC_EM}) \quad (A13)$$

$$V_{DC_EM} = V_{DC_EM_REQ} \quad (A14)$$

$$K_{DC_EM} = V_{DC_EM} / V_{ESS} \quad (A15)$$

Traction mode:

$$I_{ESS_DC} = I_{DC_EM} \times K_{DC_EM} / \eta_{DC_EM} \quad (A16)$$

Regenerative mode:

$$I_{ESS_DC} = I_{DC_EM} \times K_{DC_EM} \times \eta_{DC_EM} \quad (A17)$$

where K is the main DC-DC converter's voltage step-up factor, P is the power (W), I is the current (A), V is the voltage (V), and η is the efficiency. The $V_{DC_EM_REQ}$ in (A14) is a command sent by the EMS to the DC-DC converter to set the appropriate DC link voltage.

The output from the auxiliary DC-DC converter is given as:

$$\eta_{DC_AUX} = LuT(P_{AUX} / P_{DC_AUX}) \quad (A18)$$

$$V_{DC_AUX} = V_{DC_AUX_REQ} \quad (A19)$$

$$K_{DC_AUX} = V_{DC_AUX} / V_{ESS} \quad (A20)$$

$$I_{ESS_AUX} = I_{AUX} \times K_{DC_AUX} / \eta_{DC_AUX} \quad (A21)$$

where K is the auxiliary DC-DC converter's voltage step-down factor, P is the power (W), I is the current (A), V is the voltage (V), and η is the efficiency. $V_{DC_AUX_REQ}$ in (A19) is a command sent by the EMS to control the DC-DC converter to set the appropriate auxiliary system voltage.

The auxiliary system consists of the heating, ventilation, and air conditioning (HVAC) system and is mainly used to regulate the cabin and battery temperatures.

$$P_{AUX} = P_{OH} + P_{HVAC_CAB} + P_{HVAC_ESS} \quad (A22)$$

$$I_{AUX} = P_{AUX} / V_{DC_AUX} \quad (A23)$$

where P_{HVAC} is the power drawn by the HVAC, and P_{OH} is a minimal overhead power usage by the onboard electronics, including the lights and the doors, and is assumed to be constant, V is the voltage (V), and I is the current (A).

The equations of the thermal model block are presented here as functions and are described further in the ECO-comfort subsection:

$$[T_{CAB}, P_{HVAC_CAB}] = f(N_{PASS}, T_{AMB}, T_{SP}, RH_{AMB}, S_{DOOR}, S_{SUN}, F_{ECO}, CP_{HP}, P_{FAN}, R_{AIR}, G_{SOL}, \kappa_{BUS}) \quad (A24)$$

$$[T_{ESS}, P_{HVAC_ESS}] = f(P_{CELL_LOSS}, T_{AMB}, T_{INT}, \rho_{CELL}, L_{CELL}, H_{CELL}, W_{CELL}, N_{CELL}, C_{CELL}, HT_{SP}, CL_{SP}) \quad (A25)$$

where N is the number of entities (i.e., passengers, cells, etc.), T is the temperature ($^{\circ}\text{C}$), RH is the humidity (%), S is the state of the item (Boolean or vary between 0 and 1), F is the flag (Boolean), CP is the coefficient of performance (-), P is the power (W), R is the refresh rate (L/s), G is the solar irradiance (W/m^2), κ is the thermal conductance ($\text{W}/\text{m-K}$), ρ is the density (kg/m^3), L , H , and W represent the units of length (m), C is the specific heat ($\text{J}/\text{kg-K}$), and HT and CL represent the heating and cooling setpoints, respectively.

The overall current that is loaded from the battery can be written as:

$$I_{ESS_TOT} = I_{ESS_EM} + I_{ESS_AUX} - I_{ESS_CHG} \quad (A26)$$

$$I_{ESS_MAX_CHG} = CR_{MAX_CHG} \times CD_{CELL} \times N_{SP} \quad (A27)$$

$$I_{ESS_MAX_DSC} = CR_{MAX_DSC} \times CD_{CELL} \times N_{SP} \quad (A28)$$

$$I_{ESS} = \begin{cases} I_{ESS_TOT}, & \text{if } I_{ESS_MAX_CHG} \leq I_{ESS_TOT} \leq I_{ESS_MAX_DSC} \\ I_{ESS_MAX_CHG}, & \text{if } I_{ESS_TOT} \leq I_{ESS_MAX_CHG} \\ I_{ESS_MAX_DSC}, & \text{if } I_{ESS_TOT} \geq I_{ESS_MAX_DSC} \end{cases} \quad (A29)$$

where CR is the charging or discharging rate (-), CD is the cell capacity (Ah), N_{SP} is the number of parallel strings (-), and I is the current (A).

The output voltage of the battery, V_{ESS} , and its SoC will be presented as a function to make them independent of the battery chemistry. The output voltage, SoC, loss, and RCD of the ESS are given as:

$$[P_{LOSS}, SC_{NEW}, V_{ESS}, EQ_{NEW}] = f(T_{AMB}, I_{ESS}, SC_{CUR}, EQ_{CUR}, N_{SC}, N_{SP}, CD_{CELL}, V_{CELL_MIN}, V_{CELL_MAX}, LuT_{RS} (SC_{CUR}, CR, T_{ESS}), LuT_{RP} (SC_{CUR}, CR, T_{ESS}), LuT_{TC} (SC_{CUR}, CR, T_{ESS})) \quad (A30)$$

$$RCD = LuT(EQ_{NEW}, CR, T_{ESS}) \quad (A31)$$

where P is the battery pack power loss, SC is the SoC (%), V is the battery pack voltage (V), EQ is the number of equivalent charge/discharge cycles, T is the temperature ($^{\circ}C$), I is the current (A), N_{SC} and N_{SP} are the number of cells in series and parallel, respectively, CD is the cell capacity, CR is the charging/discharging rate, given as $CR = I_{ESS} / (CD_{CELL} * N_{SP})$, RCD is the relative capacity degradation (%), and R_s , R_p , and T_c are the series resistance, polarization resistance, and time constant, respectively.

The output of the DC charger is given as:

$$P_{ESS} = V_{ESS} \times I_{ESS_CHG} \quad (A32)$$

$$\eta_{CHG_DC} = LuT(V_{ESS}, P_{ESS}/P_{DC_RAT}) \quad (A33)$$

For grid to vehicle:

$$P_{LOAD} = P_{ESS} / \eta_{CHG_DC} \quad (A34)$$

For vehicle to grid:

$$P_{LOAD} = P_{ESS} \times \eta_{CHG_DC} \quad (A35)$$

$$V_{LOAD} = V_{ESS} / K_{CHG_DC} \quad (A36)$$

$$I_{LOAD} = P_{LOAD} / V_{LOAD} \quad (A37)$$

$$\eta_{CHG_TRN} = LuT(P_{LOAD}, R_{FLTR}) \quad (A38)$$

$$PF_{CHG_TRN} = LuT(P_{LOAD}, R_{FLTR}) \quad (A39)$$

For grid to vehicle:

$$P_{GRD_TRN} = P_{LOAD} / \eta_{CHG_TRN} \quad (A40)$$

For vehicle to grid:

$$P_{GRD_TRN} = P_{LOAD} \times \eta_{CHG_TRN} \quad (A41)$$

$$V_{AC_RMS} = V_{LOAD} \times K_{CHG_TRN} \quad (A42)$$

$$I_{GRD_TRN} = P_{GRD_TRN} / (V_{AC_RMS} \times PF_{CHG_TRN} \times \sqrt{3}) \quad (A43)$$

where K is the charger's voltage step-up or step-down factor, P is the power (W), I is the current (A), V is the voltage (V), η is the efficiency, PF is the power factor experienced by the grid, and R is the resistance (Ω) of the low-pass filter. Since the transformer interacts simultaneously with multiple chargers, the sum of the power and current are taken.

The output of the substation transformer is given as:

$$P_{GRD_TOT} = \Sigma(P_{GRD_TRN}) \quad (A44)$$

$$I_{GRD_TOT} = \Sigma(I_{GRD_TRN}) \times \sqrt{3} \quad (A45)$$

$$P_{LOAD} = I_{GRD_TOT} \times V_{AC_RMS} \quad (A46)$$

$$PF_{AVG} = P_{GRD_TOT} / P_{LOAD} \quad (A47)$$

$$\eta_{TRN} = LuT(P_{LOAD}, PF_{AVG}) \quad (A48)$$

$$P_{GRD} = P_{LOAD} / \eta_{TRN} \quad (A49)$$

$$V_{GRD_RMS} = V_{AC_RMS} \times K_{TRN} \quad (A50)$$

$$I_{GRD_RMS} = P_{GRD} / V_{GRD_RMS} \quad (A51)$$

where K is the transformer's voltage step-down factor, PF is the average power factor experienced by the grid, V is the voltage (V), I is the current (A), and η is the efficiency. The average PF is taken since each charger will present its unique PF to the transformer, but the grid will experience the average of all the chargers.

References

1. The 2 Degrees Institute. Available online: <https://www.2degreesinstitute.org/> (accessed on 15 April 2021).
2. CO₂ Emissions from Fuel Combustion: Overview—Analysis—IEA. Last Updated on July 2020. Available online: <https://www.iea.org/reports/co2-emissions-from-fuel-combustion-overview> (accessed on 15 April 2021).
3. CO₂ Emissions—Worldometer. Available online: <https://www.worldometers.info/co2-emissions/> (accessed on 15 April 2021).
4. Siddi, M. *The European Green Deal: Assessing Its Current State and Future Implementation*; Working paper # 114; Finnish Institute of International Affairs: Helsinki, Finland, 2020; ISBN 978-951-769-637-1. ISSN 2242-0444.
5. Veugelers, R.; Cincera, M.; Frietsch, R.; Schubert, T.; Rammer, C.; Pelle, A.; Renda, A.; Leijten, J.; Montalvo, C. The impact of Horizon 2020 on innovation in Europe. *Intereconomics* **2015**, *50*, 1–30. [CrossRef]
6. Home—ASSURED Project. Last Updated on 15 April 2021. Available online: <https://assured-project.eu/> (accessed on 15 April 2021).
7. Urban Mobility | Mobility and Transport. Last Updated on 7 June 2020. Available online: https://ec.europa.eu/transport/themes/urban/urban_mobility_en (accessed on 15 April 2021).
8. Kallenius, O.; Brungger, R.J.; Schafer, M. *Strategy | Livable Cities*; Daimler Sustainability Report 2019; Daimler AG: Stuttgart, Germany, 2019; pp. 50–55.
9. Hallmark, S.L.; Wang, B.; Qiu, Y.; Sperry, R. Evaluation of in-use fuel economy for hybrid and regular transit buses. *J. Transp. Technol.* **2013**, *3*, 52–57. [CrossRef]
10. Gaurs, I.; Laizans, A.; Rajekis, P.; Rubenis, A. Public Bus Energy Consumption Investigation for Transition to Electric Power and Semi Dynamic Charging. In Proceedings of the 14th International Scientific Conference Engineering for Rural Development, Jelgava, Latvia, 20–22 May 2015.
11. Battery Bus Range—It's all in the Math | Mass Transit Mag. Last Updated on 27 October 2015. Available online: <https://www.masstransitmag.com/bus/article/12131451/battery-bus-range-its-all-in-the-math> (accessed on 15 April 2021).
12. Wikner, E.; Thiringer, T. Extending battery lifetime by avoiding high SoC. *Appl. Sci.* **2018**, *8*, 1825. [CrossRef]
13. Bayes, K.; Kolk, M.; Carlot, F.; Merhaba, A.; Ito, Y. *Future of Batteries, Winner Takes All?* Arthur D. Little: Brussels, Belgium, 2018.
14. Mathieu, L.; Poliscanova, J.; Ambel, C.C.; Muzi, N.; Alexandridou, S. *Recharge EU: How Many Charge Points Will Europe and Its Member States Need in the 2020s*; European Federation for Transport and Environment: Brussels, Belgium, 2020.
15. Hasan, M.M.; El Baghdadi, M.; Hegazy, O. Energy Management and ECO-Strategies Modeling of Electric Bus Fleets in Cities. In Proceedings of the 23rd European Conference of Power Electronics and Applications, EPE 2021, Ghent, Belgium. under peer review.
16. Hasan, M.M.; Maas, J.; el Baghdadi, M.; de Groot, R.; Hegazy, O. Thermal Management Strategy of Electric Buses Towards ECO-Comfort. In Proceedings of the 8th Transport Research Arena Conference, TRA 2020, Helsinki, Finland, 27–30 April 2020.
17. Quak, H.; Koffrie, R.; van Rooijen, T.; Nesterova, N. *Economics of EVs for City Logistics*; FREVUE Deliverable report D3.2; Society of Automotive Engineers of Japan: Tokyo, Japan, 2017.
18. Nicholas, M. *Estimating Electric Vehicle Charging Infrastructure Costs across Major U.S. Metropolitan Areas*; International Council on Clean Transportation: San Francisco, CA, USA, 2019; Volume 14.
19. Buchmann, I. *Batteries in a Portable World: A Handbook on Rechargeable Batteries for Non-Engineer*, 4th ed.; Cadex Electronics: Richmond, BC, Canada, 2017; ISBN 978-0968211847.

20. Hasan, M.M.; Ranta, M.; El Baghdadi, M.; Hegazy, O. Charging Management Strategy Using ECO-Charging for Electric Bus Fleets in Cities. In Proceedings of the 2020 IEEE Vehicle Power and Propulsion Conference, VPPC 2020, Gijon, Spain, 26–29 October 2020.
21. Barcelona Bus Map 2021 | Transports Metropolitans de Barcelona. Available online: <https://www.tmb.cat/en/barcelona-transport/map/bus> (accessed on 15 April 2021).
22. What Are the 5 Koppen Climate Classification Types?—Earth How. Updated on 19 January 2021. Available online: <https://earthhow.com/koppen-climate-classification/> (accessed on 15 April 2021).
23. Teknikgatan, 417 56 Göteborg, Sweden to Sven Hultins Plats—Google Maps. Available online: <https://www.google.com/maps/dir/Teknikgatan,+417+56+G%C3%B6teborg,+Sweden/Sven+Hultins+Plats,+412+58+G%C3%B6teborg,+Sweden> (accessed on 15 April 2021).
24. Eriksbergstorget to Sahlgrenska Sjukhuset—Google Maps. Available online: <https://www.google.com/maps/dir/Eriksbergstorget,+417+64+G%C3%B6teborg,+Sweden/Sahlgrenska+Sjukhuset,+Bl%C3%A5+str%C3%A5ket,+Gothenburg,+Sweden> (accessed on 15 April 2021).
25. ISO 7730:2005. *Ergonomic of Thermal Environment—Analytical Determine & Interpret of Thermal Comfort Using Calc of PMV/PPD Indices & Thermal Comfort Criteria*, 3rd ed.; ISO/TC 159/SC 5 working group under 13.180; Ergonomic: London, UK, 2005.
26. Hasan, M.M.; el Baghdadi, M.; Hegazy, O. Energy Management Strategy in Electric Buses for Public Transport Using ECO-Driving. In Proceedings of the 15th International Conference on Ecological Vehicles and Renewable Energies, EVER 2020, Monte-Carlo, Monaco, 28–30 May 2020.
27. Topic, J.; Soldo, J.; Maletic, F.; Skugor, B.; Deur, J. Virtual Simulation of Electric Bus Fleets for City Bus Transport Electrification Planning. *Energies* **2020**, *13*, 3410. [[CrossRef](#)]
28. Barraza, O.; Estrada, M. Battery electric bus network: Efficient design and cost comparison of different powertrains. *Sustainability* **2021**, *13*, 4745. [[CrossRef](#)]
29. Thomas, J.; Mahapatra, S.S. Improved simple optimization (SOPT) algorithm for unconstrained non-linear optimization problems. *Perspect. Sci.* **2016**, *8*, 159–161. [[CrossRef](#)]
30. Tolkunov, D.; Morozov, A. Single temperature for Monte Carlo optimization on complex landscapes. *Phys. Rev. Lett.* **2012**, *108*, 250602. [[CrossRef](#)] [[PubMed](#)]